

Fall 2021

Impact of Graphene on Microstructure and Compressive Strength of Cement Mortars Utilizing Two Different Dispersion Methods

Elhussien Khaled Elbatanouny

Follow this and additional works at: <https://scholarcommons.sc.edu/etd>



Part of the [Civil Engineering Commons](#)

Recommended Citation

Elbatanouny, E. K.(2021). *Impact of Graphene on Microstructure and Compressive Strength of Cement Mortars Utilizing Two Different Dispersion Methods*. (Master's thesis). Retrieved from <https://scholarcommons.sc.edu/etd/6596>

This Open Access Thesis is brought to you by Scholar Commons. It has been accepted for inclusion in Theses and Dissertations by an authorized administrator of Scholar Commons. For more information, please contact digres@mailbox.sc.edu.

IMPACT OF GRAPHENE ON MICROSTRUCTURE AND COMPRESSIVE STRENGTH OF
CEMENT MORTARS UTILIZING TWO DIFFERENT DISPERSION METHODS

by

Elhussien Khaled Elbatanouny

Bachelor of Science
Helwan University, 2017

Submitted in Partial Fulfillment of the Requirements

For the Degree of Master of Science in

Civil Engineering

College of Engineering and Computing

University of South Carolina

2021

Accepted by:

Paul Ziehl, Director of Thesis

Sarah Gassman, Reader

Fabio Matta, Reader

Tracey L. Weldon, Interim Vice Provost and Dean of the Graduate School

© Copyright by Elhussien Khaled Elbatanouny, 2021
All Rights Reserved.

DEDICATION

This thesis is dedicated to my family, fiancée, and friends for their love, support, and encouragement. To my professors at the University of South Carolina and Helwan University.

ACKNOWLEDGEMENTS

I would like to express my deepest appreciation to my advisor, Dr. Ziehl, for his time and support during this research. Without his guidance, this thesis would not have been possible.

I would like to thank my committee members, Dr. Sarah Gassman and Dr. Fabio Matta, for their support throughout my research and for serving on my thesis committee.

I would like to thank Mr. Edward Deaver of Holcim Cement for his invaluable advice and help throughout my research.

I would like to thank the members of my department, Civil and Environmental Engineering, that helped me during this journey.

Finally, thanks to God, “Allah”.

ABSTRACT

Carbon-based nanomaterials are currently used to reinforce cement-based composite materials based on their superior properties. This study investigates the mechanical property (compressive strength) of cement mortars incorporated with pristine graphene. The dosages of graphene materials used were 0.01%, 0.02%, 0.03%, and 0.04% by weight of cement. Moreover, this study compares two dispersion techniques: ultrasonication with surfactant coating and mechanical blending with surfactant coating to promote the use of graphene in cement mortars. A commonly used polycarboxylate superplasticizer Sika-Viscocrete Ultra 2100, was used as a dispersant agent (surfactant) of graphene with a surfactant to graphene weight ratio of 9 to 1. Dynamic Light Scattering analysis was used to assess graphene aqueous suspensions and obtain the optimum surfactant to graphene weight ratio. The 28-day compressive strength of the cement mortars containing pristine graphene with 0.03% by weight of cement was enhanced by 38% and 33.6% for ultrasonication with surfactant coating and mechanical blending with surfactant coating employed as dispersion techniques of graphene, respectively, compared to the control samples. However, the mechanical blending with surfactant coating is more convenient in terms of practicality and cost than ultrasonication with surfactant coating. The workability of cement mortars incorporated with pristine graphene at these dosages was investigated. Results show that graphene, at these dosages, did not impact the workability of cement mortars. Finally, a Scanning Electron Microscope was utilized to

characterize graphene and to assess the microstructure of the cement mortars incorporated with graphene

TABLE OF CONTENTS

DEDICATION	iii
ACKNOWLEDGEMENTS.....	iv
ABSTRACT.....	v
LIST OF TABLES.....	x
LIST OF FIGURES	xi
LIST OF ABBREVIATIONS.....	xiii
CHAPTER 1: INTRODUCTION.....	1
1.1 BACKGROUND.....	1
1.2 RESEARCH SIGNIFICANCE	3
1.3 OBJECTIVES.....	4
1.4 LAYOUT OF THESIS.....	5
1.5 REFERENCES	5
CHAPTER 2: LITERATURE REVIEW	9
2.1 INTRODUCTION.....	9
2.2 MECHANICAL PROPERTIES.....	10

2.3 DISPERSION OF GRAPHENE	14
2.4 REFERENCES	17
2.5 FIGURES	21
CHAPTER 3: EXPERIMENTAL PROGRAM.....	22
3.1 MATERIALS.....	22
3.2 METHODS	23
3.3 EXPERIMENTAL PROCEDURES.....	26
3.4 REFERENCES	28
3.5 TABLES	28
3.6 FIGURES	30
CHAPTER 4: RESULTS AND DISCUSSIONS	34
4.1 INTRODUCTION.....	34
4.2 WORKABILITY OF CEMENT MORTARS.....	35
4.3 OPTIMUM SURFACTANT TO GRAPHENE WEIGHT RATIO	35
4.4 DLS ANALYSIS OF GRAPHENE AQUEOUS SUSPENSIONS	36
4.5 COMPRESSIVE STRENGTH.....	36

4.6 MICROSTRUCTURE OF CEMENT MORTARS	38
4.7 COST ANALYSIS.....	39
4.8 TABLES	40
4.9 FIGURES	41
CHAPTER 5: SUMMARY AND CONCLUSIONS.....	51
5.1 SUMMARY AND CONCLUSIONS.....	51
5.2 RECOMMENDATIONS FOR FUTURE WORK	52
REFERENCES	53
APPENDIX A : SUPPORTING MATERIALS FOR CHAPTER 4	60

LIST OF TABLES

Table 3.1 Sieve analysis for sand.....	28
Table 3.2 Physical and chemical properties of pristine graphene.....	29
Table 3.3 Properties of Superplasticizer	29
Table 3.4 Quantity of materials for compression test.....	29
Table 4.1 Average Compressive Strength for mortar batches	40
Table 4.2 Cost analysis for mortar batches.....	40
Table A.1 Compression test results for all specimens of different batches	60
Table A.2 Cost of the materials	61

LIST OF FIGURES

Figure 2.1 AHR values for aqueous dispersions (Zohhadi et al., 2014).....	21
Figure 3.1 Particle size distribution curve for sand	30
Figure 3.2 As received graphene powder	31
Figure 3.3 Sika-ViscoCrete 2100 (polycarboxylate superplasticizer)	31
Figure 3.4 The process of preparation of graphene aqueous suspensions	31
Figure 3.5 Ultrasonication Setup	32
Figure 3.6 Flow Table.....	32
Figure 3.7 Compression Test Setup	33
Figure 4.1 Flow of cement mortars with 0% and 0.04% graphene BWOC.....	41
Figure 4.2 AHR values of graphene suspensions with a different surfactant to ratio	41
Figure 4.3 AHR values of graphene suspensions before and after ultrasonication	42
Figure 4.4 Average compressive strength of the mortar batches tested	42
Figure 4.5 Stress-Strain curves for BG1 reinforced mortar cubes.....	43
Figure 4.6 Stress-Strain curves for BG2 reinforced mortar cubes.....	43
Figure 4.7 Stress-Strain curves for BG3 reinforced mortar cubes.....	44
Figure 4.8 Stress-Strain curves for BG4 reinforced mortar cubes.....	44
Figure 4.9 Stress-Strain curves for SG1 reinforced mortar cubes	45
Figure 4.10 Stress-Strain curves for SG2 reinforced mortar cubes	45
Figure 4.11 Stress-Strain curves for SG3 reinforced mortar cubes	46
Figure 4.12 Stress-Strain curves for SG4 reinforced mortar cubes	46

Figure 4.13 Comparison between the dispersion methods at each graphene dosage	47
Figure 4.14 SEM micrograph of as-received graphene powder	47
Figure 4.15 SEM micrograph showing the aggregation of as-received graphene	48
Figure 4.16 Microstructure of plain cement mortar	48
Figure 4.17 Microstructure of mortar mix containing 0.02% graphene	49
Figure 4.18 Microstructure of mortar mix containig 0.03% graphene	49
Figure 4.19 Hydration products in mortar mix containing 0.03% graphene	50
Figure 4.20 Agglomeration of graphene sheets in mortar mix at 0.04% concentration	50

LIST OF ABBREVIATIONS

BG	Mechanical blending with surfactant coating
BWOC	By weight of cement
CNTs	Carbon Nanotubes
DLS	Dynamic Light Scattering
G	Pristine Graphene
PC	Polycarboxylate
SEM	Scanning Electron Microscope
SG	Ultrasonication with surfactant coating

CHAPTER 1

INTRODUCTION

1.1 BACKGROUND

Cement-based composite materials such as cement paste, mortar, and concrete are the most well-known and universally used building materials. However, the limited strength, durability, and increasing maintenance cost, as well as the quasi-brittle nature associated with crack initiation and propagation, low toughness, and low tensile strength are major drawbacks of cement-based composite materials (Raki et al., 2010). The inherent brittleness is responsible for the low cracking resistance of cement-based composite materials. This comes from the inferior characteristics of the cement pastes in the hardened state (Pan et al. 2015). Low tensile strength and low toughness are due to internal flaws and the insufficient strain capacity of the cement (Tragazikis et al., 2019). Such limitations have been under the scope of research for some time.

Several studies have been conducted to enhance the strength and durability of concrete. The studies employ various methods such as incorporating reinforcing materials or reducing water to binder ratio by using chemical mineral admixtures. The former is the simplest reinforcing method. It utilizes different reinforcing phases including microscale dimensions such as fibers (Holschemacher et al. 2010 and Watanabe et al. 2010), or macro dimensions, such as steel bars (Rahal and Rumaih, 2011). It was concluded that improvement of the cement composite strength (concrete), as a whole, occurred due to

these reinforcing methods. However, the high brittleness and cracks still happen as the microstructure of the cement paste was not affected by the addition of the reinforcing materials. On the other hand, reducing the water to binder ratio using chemical admixtures can change the microstructure of the cement paste by decreasing the capillary voids. As a result, the mechanical strength was enhanced (Anagnostopoulos 2014 and Hu et al. 2014). However, this method cannot go beyond the minimum required water binder ratio for the hydration process.

Cracks and holes are produced in the cement paste during the hydration process (Cao et al., 2013). The main reason is that the cement paste consists of cement hydration products of ettringite (AFt), monosulfate (AFm), calcium hydroxide (CH), and calcium silicate hydrate (C-S-H) gel (Baquerizo et al. 2015). As the cement hydrates, voids are left in the paste structure due to random growth and different types of crystals. For example, CH, Aft, and AFm usually exhibit rod-like and needle-like crystals (Chakraborty et al., 2013). Interlayer hydration space and capillary voids are the two types of voids formed during the hydration process. Interlayer hydration space occurs between the layers in the C-S-H gel, and the thickness is 0.5 nm and 2.5 nm. At the same time, Capillary voids are the result of the hydrated cement having a lower bulk specific gravity than the cement particles and excess water. The initial separation of cement particles, controlled by the water to cement ratio, controls the amount and size of capillary voids. A highly hydrated cement with a minimum amount of water can have capillary voids on the order of 10 nm to 50 nm.

In contrast, a poorly hydrated cement with excess water can have capillary voids on the order of 3 μ m to 5 μ m. Capillary voids greater than 50 nm decrease strength and

increase permeability. Hence, to improve the strength of cement-based composite materials, especially the flexural/tensile strength, regulating the shape of hydration products is required (Lv et al., 2014). The mechanical strength of the cement paste is developed from the high specific area and adhesive property of the structure of C-S-H (Chuah et al., 2014). Moreover, Stynoski et al. (2015) suggested that if nanoscale cracks can be successfully controlled, their growth to the micro-level is likely to be halted.

Recently, to address the challenges above by novel approaches, research has focused on the evolution of nanomaterials, especially carbon-based, being used as a reinforcement to the cement-based composite materials. The nanomaterials improve the mechanical performance of cement-based composite materials through two mechanisms. First, they have large specific areas, so they act as nucleation sites for the growth of hydration crystals, which increases the fraction of hydrated cement (Lv et al., 2013). Second, nanomaterials densify the microstructure, since their size is analogous to the C-S-H gel pore in the cement matrix (Pan et al., 2015). As a result, the cracks are mitigated at the nano/micro-scale. However, the dispersion of nanomaterials in cement-based composite materials is an obstacle (Tong et al., 2016). Therefore, all the beneficial impacts caused by nanomaterials may not be achieved unless they are uniformly dispersed in the matrix (Du et al., 2015).

1.2 RESEARCH SIGNIFICANCE

There is currently a lack of knowledge concerning the degree of improvement of the mechanical properties that can be achieved with the addition of dosages (0.01% to 0.04% by weight of cement) of pristine graphene into cement-based composite materials. Specifically, to the author's knowledge, information is highly scarce in the literature

concerning the effect of pristine graphene, at these dosages, presence on the compressive strength of cement. It is almost exclusively limited to the paste form of the material. Furthermore, no standards or specifications can be followed for the dispersion of pristine graphene in cement-based composite materials. Recently, polycarboxylate superplasticizers have been commonly used as a dispersant agent with the help of mechanical methods such as ultrasonication, shear mixing, or mechanical blending. However, researchers focused on the effect of different commonly used polycarboxylate superplasticizers with the help of the same mechanical method as the work done by Papanikolaou et al. (2021).

This study investigates the effect of incorporating pristine graphene (G) into cement mortars using two different dispersion methods. First, dosages of G by weight of cement (BWOC) are tested to show the impact on cement mortars. Second, the commonly used polycarboxylate superplasticizer (Sika Viscocrete 2100) is used as a dispersant agent with the help of two different mechanical methods: ultrasonication and mechanical blending.

1.3 OBJECTIVES

The two main objectives of this study were to determine the effect of the addition of G on the mechanical strength of the cement mortars and to compare the two different methods employed for the dispersion of G in cement mortars with the help of the polycarboxylate superplasticizer (Sika ViscoCrete 2100) as a dispersant agent. These can be accomplished as follows:

- 1- Determine the percent increase in compressive strength due to different dosages of graphene added to cement mortars.

- 2- Plot the stress-strain curve for the tested specimens due to different dosages of graphene added to cement mortars.
- 3- For the exact dosages of graphene, determine the difference between the two methods employed for dispersing graphene by comparing the results of the compression tests on graphene reinforced cement mortars.
- 4- Compare the Scanning Electron Microscope (SEM) results between plain cement mortars and the different dosages of graphene reinforced cement mortars.

1.4 LAYOUT OF THESIS

This thesis consists of five chapters. In Chapter 2 a literature review on the mechanical properties of graphene reinforced cement composites and the dispersion of graphene in cement-based composite materials are discussed. Background information for selected relevant studies is presented.

In Chapter 3, the experimental program conducted at the University of South Carolina Materials and Structural Engineering Laboratory is presented. After that, results and discussions of the tests are presented in Chapter 4. Chapter 5 contains a summary of the thesis and the conclusions made based on the study. Also, recommendations for future research are included in this chapter.

1.5 REFERENCES

Anagnostopoulos, C. A. (2014). Effect of different superplasticisers on the physical and mechanical properties of cement grouts. *Construction and Building Materials*, 50, 162-168.

- Baquerizo, L. G., Matschei, T., Scrivener, K. L., Saeidpour, M., & Wadsö, L. (2015). Hydration states of AFm cement phases. *Cement and Concrete Research*, 73, 143-157.
- Cao, M., Zhang, C., & Wei, J. (2013). Microscopic reinforcement for cement based composite materials. *Construction and Building Materials*, 40, 14-25.
- Chakraborty, S., Kundu, S. P., Roy, A., Adhikari, B., & Majumder, S. B. (2013). Effect of jute as fiber reinforcement controlling the hydration characteristics of cement matrix. *Industrial & Engineering Chemistry Research*, 52(3), 1252-1260.
- Chuah, S., Pan, Z., Sanjayan, J. G., Wang, C. M., & Duan, W. H. (2014). Nano reinforced cement and concrete composites and new perspective from graphene oxide. *Construction and Building Materials*, 73, 113-124.
- Du, H., & Dai Pang, S. (2015). Enhancement of barrier properties of cement mortar with graphene nanoplatelet. *Cement and Concrete Research*, 76, 10-19.
- Holschemacher, K., Mueller, T., & Ribakov, Y. (2010). Effect of steel fibres on mechanical properties of high-strength concrete. *Materials & Design (1980-2015)*, 31(5), 2604-2615.
- Hu, J., Ge, Z., & Wang, K. (2014). Influence of cement fineness and water-to-cement ratio on mortar early-age heat of hydration and set times. *Construction and building materials*, 50, 657-663.

- Lv, S., Liu, J., Sun, T., Ma, Y., & Zhou, Q. (2014). Effect of GO nanosheets on shapes of cement hydration crystals and their formation process. *Construction and Building Materials*, 64, 231-239.
- Lv, S., Ma, Y., Qiu, C., Sun, T., Liu, J., & Zhou, Q. (2013). Effect of graphene oxide nanosheets of microstructure and mechanical properties of cement composites. *Construction and building materials*, 49, 121-127.
- Pan, Z., He, L., Qiu, L., Korayem, A. H., Li, G., Zhu, J. W., ... & Wang, M. C. (2015). Mechanical properties and microstructure of a graphene oxide–cement composite. *Cement and Concrete Composites*, 58, 140-147.
- Papanikolaou, I., de Souza, L. R., Litina, C., & Al-Tabbaa, A. (2021). Investigation of the dispersion of multi-layer graphene nanoplatelets in cement composites using different superplasticiser treatments. *Construction and Building Materials*, 293, 123543.
- Rahal, K. N., & Rumaih, H. A. (2011). Tests on reinforced concrete beams strengthened in shear using near surface mounted CFRP and steel bars. *Engineering Structures*, 33(1), 53-62.
- Raki, L., Beaudoin, J., Alizadeh, R., Makar, J., & Sato, T. (2010). Cement and concrete nanoscience and nanotechnology. *Materials*, 3(2), 918-942.
- Stynoski, P., Mondal, P., & Marsh, C. (2015). Effects of silica additives on fracture properties of carbon nanotube and carbon fiber reinforced Portland cement mortar. *Cement and Concrete Composites*, 55, 232-240.

- Tong, T., Fan, Z., Liu, Q., Wang, S., Tan, S., & Yu, Q. (2016). Investigation of the effects of graphene and graphene oxide nanoplatelets on the micro-and macro-properties of cementitious materials. *Construction and Building Materials*, 106, 102-114.
- Tragazikis, I. K., Dassios, K. G., Dalla, P. T., Exarchos, D. A., & Matikas, T. E. (2019). Acoustic emission investigation of the effect of graphene on the fracture behavior of cement mortars. *Engineering Fracture Mechanics*, 210, 444-451.
- Watanabe, K., Kimura, T., & Niwa, J. (2010). Synergetic effect of steel fibers and shear-reinforcing bars on the shear-resistance mechanisms of RC linear members. *Construction and Building Materials*, 24(12), 2369-23

CHAPTER 2

LITERATURE REVIEW

2.1 INTRODUCTION

Materials that are less than 100 nanometers in one of their dimensions are known as nanomaterials. According to their scale or morphology, they are classified into three types, nanoparticles (0D), nanofibers (1D), and nanosheets (2D). Nanoparticles such as nano silica (nano SiO₂) have an approximate average size of 9 nm and a specific surface area of 300 m²/g with a spherical shape (low aspect ratio) (Senff et al. 2009). Li et al. (2004) investigated the effect of adding nanoparticles to cement mortars. The dosages of nano SiO₂ studies were 3%, 5%, and 10% by weight of cement. They reported that adding nano SiO₂ by 5% to cement mortars resulted in a 26% increase of compressive strength compared to plain cement mortars. In comparison, adding 10% nano SiO₂ resulted in a 27% increase in flexural strength.

Nanofibers (1D) such as carbon nanotubes (CNTs) have an approximate average size of 15-40 nm with a one-dimension tube shape, tensile strength with a range of 11-63 GPa, a specific surface area 700-1500 m²/g, and a high aspect ratio equal to 1000 (Yu et al., 2000 and Peigney et al., 2001). On the other hand, nanosheets such as graphene have a high specific area of 2600 m²/g for single-layer graphene with a two-dimensional sheet shape, an average thickness of 0.08 nm, and a high aspect ratio with a range of 6000-600,000 (Stankovich et al., 2006 and Chuah et al., 2014). Their large surface area

guarantees a strong bond between them and the cement matrix due to the strong Van der Waals forces inhibiting the formation and propagation of microcracks superior to nanoparticles (Meng and Khayat, 2018). Graphene will allow the realization of contact areas with the surrounding medium, doubling the contact area by CNTs. Hence, a smaller amount of graphene content is required to match the performance enhancement offered by CNTs, making graphene hierarchically superior to CNTs. According to the material properties of nanofibers (1D) and nanosheets (2D). A small amount of these materials (in proportion to the weight of cement) can inhibit crack initiation at the nanoscale and fill the voids in the cement paste matrix, improving the mechanical properties of the cement-based composite materials (Meng and Khayat, 2016). Several studies confirmed this, while others had contrasting results. This contradiction in results is due to the tendency of nanofibers and nanosheets to agglomerate in the cement matrix. A good dispersion of these nanomaterials, especially nanosheets such as graphene, can significantly improve the mechanical strength and durability of cement-based composite materials.

2.2 MECHANICAL PROPERTIES

2.2.1 Properties of graphene and its derivatives

In 2004, by way of mechanical exfoliation from graphite, two-dimensional carbon-based material graphene was discovered by Andre Geim and Konstantin Novoselov (Novoselov et al., 2004). Graphene is the most robust material ever to be measured using nanoindentation atomic force microscopy with a young's modulus of 1 TPa and a very high tensile strength of 130 GPa (Lee et al., 2008). Additionally, Graphene has also high thermal conductivity ($5000 \text{ Wm}^{-1}\text{K}^{-1}$) and high electronic mobility ($200000 \text{ cm}^2\text{V}^{-1}\text{S}^{-1}$) (Balandin et al., 2008 and Bolotin et al., 2008). Graphene shows better properties than its derivatives

graphene oxide (GO) and reduced graphene oxide (rGO). GO is composed of graphene layers with active oxygen-containing functional groups on its surface. Compared to pristine graphene, GO has a low electrical conductivity limiting the smart functionality like strain/damage sensing ability (Zheng et al., 2017). Dikin et al. (2007) reported that the elastic modulus of GO is approximately 32 GPa, while its tensile strength is 130 GPa (Zhu et al., 2010), and its surface area is around 700 m²/g (Montes-Navajas et al., 2013). rGO properties lie between Graphene and GO. Therefore, Graphene is superior to its derivatives. However, due to the oxygen functional groups on its surface, (GO) is hydrophilic and easily dispersed in water, while pristine graphene is hydrophobic, making it easier to incorporate GO in cement-based composite materials (Qureshi and Panesar, 2020).

2.2.2 Graphene reinforced cement-based composite materials

Several studies were conducted, considering graphene's outstanding properties to determine the effect of pristine graphene on cement-based composite materials. Qureshi and Panesar (2020) compared cement pastes incorporated with functionalized graphene (GO and rGO) and pristine graphene nanoplatelets (G). The authors examined the workability, hydration, microstructure, and mechanical properties of cement pastes. The dosage of graphene materials was 0.01%, 0.02%, 0.04%, 0.08%, and 0.16% by weight of cement. The maximum 28-day compressive and flexural strength of (GO, rGO and G) were 28% and 81% at 0.02% GO, 30% and 84% at 0.04% rGO, and 39% and 38% at 0.02 G, greater than the control sample (without graphene), respectively. Moreover, as the percentage of GO increased, the workability of the cement paste decreased, while rGO and G had a minor impact on the workability. Also, the incorporation of graphene materials densifies and reinforces the microstructure. As well, Wang et al. (2016) tested the

compressive and flexural strength of cement pastes at curing ages of 3, 7, 14, and 28 days with the addition of 0.05% graphene by weight of cement. The compressive strength and flexural strength increased as the age increases. However, at an early age, the introduction of graphene dramatically enhances the strength of the cement paste. At seven days, the flexural and the compressive strength increased by 23.5% and 7.5%, respectively, while at 28 days, they had increased by 16.8% and 1.3%, respectively, compared to the blank sample without graphene.

Building on the results from cement pastes, I.K. Tragazikis et al. (2019) examined the effect of graphene on the mechanical response of cement mortars. The dosage of graphene inspected was 0.2% and 0.4% by weight of cement. The impact of graphene content increased the compression strength by 8% and 13% for 0.2% and 0.4%, respectively, compared to the control sample (no graphene). Nevertheless, the flexural strength decreased by 42% and 27%, respectively, with 0.2% and 0.4%. Also, using the same materials and dosage of graphene as Tragazikis et al. (2019), Dalla et al. (2021) reported an increase in the compression strength by 14% and 18% for 0.2% and 0.4%, respectively, in comparison with the control sample (no graphene), while the flexural strength decreased by 21.5% and 14% with 0.2% and 0.4% respectively. Further, Sharma and Arora (2017) reported incorporating graphene into fly ash cement mortars at different doses: 0.05% and 0.1% by weight of cement. They used fine recycled aggregates (FRA) as a replacement for fine natural aggregates (FNA). The specimens were tested at curing times of 28, 60, 90, and 120 days. Hence, 0.05% graphene and FRA caused an increase of 8% and 13% in the compressive strength and flexural strength, respectively, with respect to FNA mortar without graphene after 120 days of curing. The compressive and flexural

strength increased as the curing age increase. However, 0.1% graphene and FRA caused a decrease by 3.4% and 4% in the compressive strength and flexural strength, respectively, with respect to FNA mortar without graphene after 120 days of curing.

Based on the studies mentioned above, it was noticed that the addition of graphene at low dosages such as 0.01% to 0.04% showed good results on the mechanical strength of the cement-based composite materials, with limited literature only on the cement paste. However, only one study has investigated the effect of these dosages on cement mortars, but only on the early flexural strength with one dispersion method. Li et al. (2018) investigated the microstructure and the early flexural strength (3 and 7 days) with a three-point bending test of graphene reinforced cement mortars. The dosage of graphene varied from 0.01% to 0.05% by weight of cement. At 0.03% of graphene-modified cement mortars, the early flexural strength at seven days increased by 40% in comparison to the control sample.

2.2.3 Graphene oxide reinforced cement-based composite materials

Preceding studies reported that GO could enhance the mechanical performance and the durability of cement-based composite materials. The addition of GO to cement-based composite materials at very low dosages, such as 0.01% to 0.04%, has been investigated by various researchers. Mokhtar et al. (2017) conducted a study to examine the effect of adding GO on the mechanical and microstructure of cement pastes. Five different batches were cast with varying dosages of GO 0.01%, 0.02%, 0.03%, 0.04%, and 0.05% by weight of cement with the fifth being a control batch of ordinary cement paste. The authors reported a significant reduction in the pore size and enhancement in the microstructure with the lowest intensity in the pore size distribution at 0.02% of GO. Accordingly, they reported

the maximum increase of compressive strength was 13% higher at 0.02% GO than the control batch. Moreover, Indukuri and Nerella (2021) determined the effect of adding GO to cement paste on the mechanical properties at low dosages such as 0.01%, 0.02%, 0.03%, and 0.04% by weight of cement. They concluded that the maximum increase in compressive and flexural strength was at 0.03% GO, which is 46% and 77.7% higher, respectively, than the control cement paste.

Lv et al. (2013) determined the effect of GO nanosheets on the mechanical properties of cement mortars. Five different batches were prepared with varying dosages of GO 0.01%, 0.02%, 0.03%, 0.04%, and 0.05% by weight of cement and a control batch with no addition of GO. The results showed that when the cement composites with the content of GO (0.03%), the tensile, flexural, and compressive strength were 78.6%, 60.7%, and 38.9% more than the control batch with no addition of GO. Building on the previous results, Lv et al. (2014) investigated the effect of GO nanosheets on cement hydration products. They concluded that rod-like crystals produced from cement hydration changed to flower-like crystals at a low dosage of GO (<0.03%), while it changed into a polyhedral at a high dosage of GO (>0.03%), proving that the addition of GO altered the formation and properties of the cement hydration crystals. Comparing the results between the two studies (Lv et al. 2013 and Lv et al. 2014), at 0.03% on mortars, the compressive and flexural strength increased by 38.9% and 60.7% (Lv et al., 2013), while on cement pastes, the compressive and flexural strength increased by 20.1% and 27.3% (Lv et al., 2014).

2.3 DISPERSION OF GRAPHENE

The great benefits of presenting graphene nano-reinforcement in the cement-based composites can be limited by the poor graphene dispersion in the cement matrix, as it

results in defects due to the agglomeration of graphene sheets (Sixuan, 2012). In addition, graphene is hydrophobic and tends to agglomerate and precipitate in water. Therefore, mechanical and chemical methods were adopted to disperse the nanomaterials in the cement matrix. High-speed shear mixing, ultrasonication, and mechanical blending were utilized as the mechanical methods. On the other hand, surfactants, surfactant modification aids, or acid-etching were used as chemical methods. As a result, three dispersion techniques were adopted to disperse graphene in the cement matrix (Lin and Du, 2020).

First, the dry dispersion technique is employed by mixing graphene with dry cement using high-speed shear mixing or an electric mixer. However, Jing et al. (2017) tested this method, and the results showed no difference in the degree of cement hydration reaction due to the poor dispersion and agglomeration of graphene. Second, for the wet dispersion technique, with the help of mechanical stirring and the use of surfactants, Li et al. (2018) prepared graphene cement mortars by mixing cement, sand, graphene, water, and a polycarboxylate superplasticizer. The microstructure of graphene reinforced cement mortars was investigated. The researchers observed that a 3-D structure was formed as graphene sheets connected with ettringite, C-S-H gel, and other crystals. The 3-D structure bridged cracks and filled the pores making the cement matrix stronger and tougher. Finally, the most commonly used technique is the wet dispersion technique, which is performed with the help of mechanical stirring, ultrasonication, and surfactants. Water, graphene, and surfactant were mixed, then ultrasonicated to obtain a uniformly dispersed graphene solution. After that, the solution was mixed with the cement matrix.

Zohhadi et al. (2015) investigated the effects of three dispersion techniques for graphene reinforced cement composites. First, graphene aqueous suspensions were

prepared by employing ultrasonication referred to as (u-GNP), surfactant coating with the help of ultrasonication (s-GNP), and acid-etching (a-GNP). They used the anionic surfactant sodium deoxycholate (NADC) as a surfactant. Second, Dynamic Light Scattering (DLS) analyses were used to assess the stable dispersion of the graphene aqueous suspensions by comparing the average hydrodynamic radius (AHR) values of the aqueous suspensions. The lower the AHR value, the higher the level of dispersion of the graphene aqueous suspensions. Zohhadi et al. (2015) reported that the AHR values of the u-GNP, a-GNP, and s-GNP aqueous suspensions were 215 nm, 166 nm, and 55 nm, respectively. Therefore, surfactant coating, with the help of ultrasonication, provided the highest level of dispersion.

Papanikolaou et al. (2021) investigated the dispersion of multi-layer graphene nanoplatelets in cement composites using different superplasticizer treatments by zeta potential measurements, rheology, and UV-Visible spectroscopy. First, the four commonly used superplasticizers were tested, including a lignosulphonate, a naphthalene-based polycarboxylate ether, and modified polycarboxylic ether with the help of sonication. In addition, they tried the dispersion of graphene in water with sonication only and with sonication and surfactants. They concluded that both sonication and surfactants are necessary to ensure that graphene is homogeneously dispersed. Additionally, polycarboxylate superplasticizers that work by steric hindrance mechanism were more effective than lignosulphonate and naphthalene-based that work by electrostatic repulsion to achieve a homogeneous and stable dispersion of graphene. This agrees with Zhao et al. (2018), who showed that polycarboxylate superplasticizer was more efficient than

lignosulfonate and polycondensate naphthalene sulfonate formaldehyde as confirmed by zeta potential and transmission electron microscope (TEM).

2.4 REFERENCES

Balandin, A. A., Ghosh, S., Bao, W., Calizo, I., Teweldebrhan, D., Miao, F., & Lau, C. N. (2008). Superior thermal conductivity of single-layer graphene. *Nano letters*, 8(3), 902-907.

Bolotin, K. I., Sikes, K. J., Jiang, Z., Klima, M., Fudenberg, G., Hone, J., ... & Stormer, H. L. (2008). Ultrahigh electron mobility in suspended graphene. *Solid state communications*, 146(9-10), 351-355.

Chuah, S., Pan, Z., Sanjayan, J. G., Wang, C. M., & Duan, W. H. (2014). Nano reinforced cement and concrete composites and new perspective from graphene oxide. *Construction and Building Materials*, 73, 113-124.

Dalla, P. T., Tragazikis, I. K., Trakakis, G., Galiotis, C., Dassios, K. G., & Matikas, T. E. (2021). Multifunctional Cement Mortars Enhanced with Graphene Nanoplatelets and Carbon Nanotubes. *Sensors*, 21(3), 933.

Dikin, D. A., Stankovich, S., Zimney, E. J., Piner, R. D., Dommett, G. H., Evmenenko, G., ... & Ruoff, R. S. (2007). Preparation and characterization of graphene oxide paper. *Nature*, 448(7152), 457-460.

Indukuri, C. S. R., & Nerella, R. (2021). Enhanced transport properties of graphene oxide-based cement composite material. *Journal of Building Engineering*, 37, 102174.

- Jing, G., Ye, Z., Lu, X., & Hou, P. (2017). Effect of graphene nanoplatelets on hydration behaviour of Portland cement by thermal analysis. *Advances in Cement Research*, 29(2), 63-70.
- Lee, C., Wei, X., Kysar, J. W., & Hone, J. (2008). Measurement of the elastic properties and intrinsic strength of monolayer graphene. *science*, 321(5887), 385-388.
- Li, G., Yuan, J. B., Zhang, Y. H., Zhang, N., & Liew, K. M. (2018). Microstructure and mechanical performance of graphene reinforced cementitious composites. *Composites Part A: Applied Science and Manufacturing*, 114, 188-195.
- Li, H., Xiao, H. G., Yuan, J., & Ou, J. (2004). Microstructure of cement mortar with nanoparticles. *Composites part B: engineering*, 35(2), 185-189.
- Lin, Y., & Du, H. (2020). Graphene reinforced cement composites: A review. *Construction and Building Materials*, 265, 120312.
- Lv, S., Liu, J., Sun, T., Ma, Y., & Zhou, Q. (2014). Effect of GO nanosheets on shapes of cement hydration crystals and their formation process. *Construction and Building Materials*, 64, 231-239.
- Lv, S., Ma, Y., Qiu, C., Sun, T., Liu, J., & Zhou, Q. (2013). Effect of graphene oxide nanosheets of microstructure and mechanical properties of cement composites. *Construction and building materials*, 49, 121-127.

- Lv, W., Li, Z., Deng, Y., Yang, Q. H., & Kang, F. (2016). Graphene-based materials for electrochemical energy storage devices: opportunities and challenges. *Energy Storage Materials*, 2, 107-138.
- Meng, W., & Khayat, K. H. (2016). Mechanical properties of ultra-high-performance concrete enhanced with graphite nanoplatelets and carbon nanofibers. *Composites Part B: Engineering*, 107, 113-122.
- Meng, W., & Khayat, K. H. (2018). Effect of graphite nanoplatelets and carbon nanofibers on rheology, hydration, shrinkage, mechanical properties, and microstructure of UHPC. *Cement and Concrete Research*, 105, 64-71.
- Mokhtar, M. M., Abo-El-Enein, S. A., Hassaan, M. Y., Morsy, M. S., & Khalil, M. H. (2017). Mechanical performance, pore structure and micro-structural characteristics of graphene oxide nano platelets reinforced cement. *Construction and Building Materials*, 138, 333-339.
- Montes-Navajas, P., Asenjo, N. G., Santamaría, R., Menendez, R., Corma, A., & García, H. (2013). Surface area measurement of graphene oxide in aqueous solutions. *Langmuir*, 29(44), 13443-13448.
- Novoselov, K. S., Fal, V. I., Colombo, L., Gellert, P. R., Schwab, M. G., & Kim, K. (2012). A roadmap for graphene. *nature*, 490(7419), 192-200.
- Peigney, A., Laurent, C., Flahaut, E., Bacsá, R. R., & Rousset, A. (2001). Specific surface area of carbon nanotubes and bundles of carbon nanotubes. *Carbon*, 39(4), 507-514.

- Qureshi, T. S., & Panesar, D. K. (2020). Nano reinforced cement paste composite with functionalized graphene and pristine graphene nanoplatelets. *Composites Part B: Engineering*, *197*, 108063.
- Senff, L., Hotza, D., Lucas, S., Ferreira, V. M., & Labrincha, J. A. (2012). Effect of nano-SiO₂ and nano-TiO₂ addition on the rheological behavior and the hardened properties of cement mortars. *Materials Science and Engineering: A*, *532*, 354-361.
- Sharma, S., & Arora, S. (2018). Economical graphene reinforced fly ash cement composite made with recycled aggregates for improved sulphate resistance and mechanical performance. *Construction and Building Materials*, *162*, 608-612.
- Sixuan, H. (2012). Multifunctional graphite nanoplatelets (GNP) reinforced cementitious composites. *Master's Theses, National University of Singapore, Singapore, Singapore*.
- Stankovich, S., Dikin, D. A., Dommett, G. H., Kohlhaas, K. M., Zimney, E. J., Stach, E. A., ... & Ruoff, R. S. (2006). Graphene-based composite materials. *nature*, *442*(7100), 282-286.
- Tragazikis, I. K., Dassios, K. G., Dalla, P. T., Exarchos, D. A., & Matikas, T. E. (2019). Acoustic emission investigation of the effect of graphene on the fracture behavior of cement mortars. *Engineering Fracture Mechanics*, *210*, 444-451.
- Wang, B., Jiang, R., & Wu, Z. (2016). Investigation of the mechanical properties and microstructure of graphene nanoplatelet-cement composite. *Nanomaterials*, *6*(11), 200.

Yu, M. F., Lourie, O., Dyer, M. J., Moloni, K., Kelly, T. F., & Ruoff, R. S. (2000). Strength and breaking mechanism of multiwalled carbon nanotubes under tensile load. *Science*, 287(5453), 637-640.

Zheng, Q., Han, B., Cui, X., Yu, X., & Ou, J. (2017). Graphene-engineered cementitious composites: small makes a big impact. *Nanomaterials and Nanotechnology*, 7, 1847980417742304.

Zhu, Y., Murali, S., Cai, W., Li, X., Suk, J. W., Potts, J. R., & Ruoff, R. S. (2010). Graphene and graphene oxide: synthesis, properties, and applications. *Advanced materials*, 22(35), 3906-3924.

Zohhadi, N. (2014). Functionalized graphitic nanoreinforcement for cement composites.

2.5 FIGURES

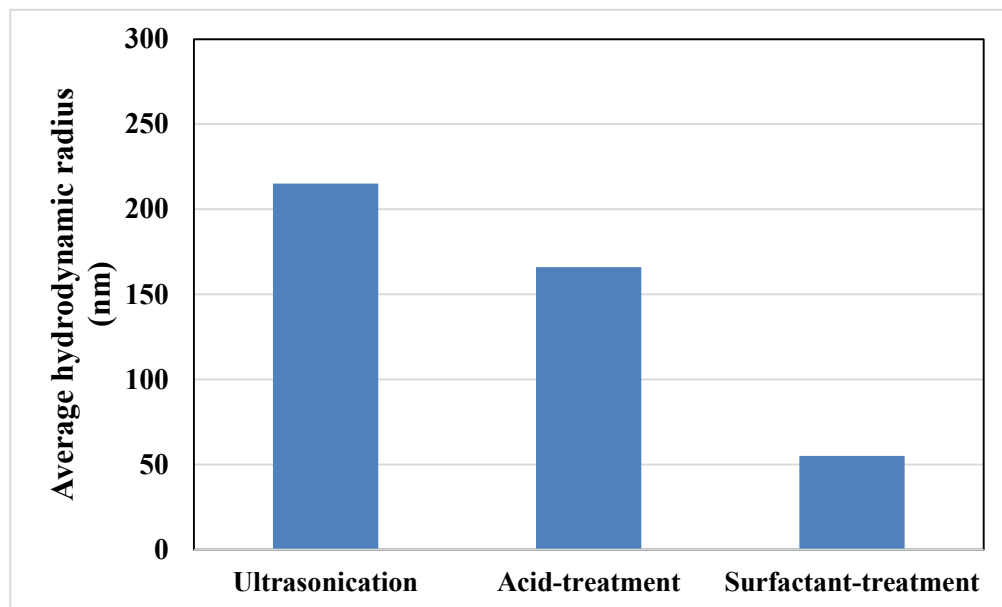


Figure 2.1 AHR values for aqueous dispersions (Zohhadi et al., 2014)

CHAPTER 3

EXPERIMENTAL PROGRAM

3.1 MATERIALS

3.1.1 Cement and mixing water

Ordinary Portland Cement (Type I) was purchased from Holcim, and regular tap water was used in this study.

3.1.2 Sand

Natural silica sand was purchased from Unimin Corporation, 1704 Gillies Creek Rd Lugoff, SC, USA. A sieve analysis test was conducted on a sample of 1375 gm of sand, and the results are shown in Table (3.1) and Figure (3.1).

3.1.3 Pristine Graphene (G)

ProCene Graphene Powder, as shown in Figure (3.2), was purchased from Proton Power Inc., Lenoir City, TN, USA. The physical and chemical properties of G are tabulated in Table (3.2) as per the product sheet.

3.1.4 Polycarboxylate Superplasticizer (PC)

SikaViscoCrete-2100, as shown in Figure (3.3), was supplied by Sika Corporation, 201 Polito Avenue, Lyndhurst, New Jersey, USA. It is a high range water reducing superplasticizer admixture used in the industry. The properties of SikaViscoCrete-2100 are shown in Table (3.3).

3.2 METHODS

3.2.1 Preparation of graphene cement mortars

The surfactant used was the commercially available polycarboxylate (PC) superplasticizer (Sika ViscoCrete 2100). The two methods employed in this study are described in the following two sections.

3.2.1.1 Mechanical Blending with surfactant coating (BG)

The pristine graphene (G) dispersion was conducted using a PC superplasticizer as a dispersant agent and blending all the mixing materials with a mechanical blender as Li et al. (2018) recommended. The cement mortar specimens were cast by employing surfactant coating (PC) and the materials were blended together with a mechanical blender. This being the dispersion method of G it is hence forth referred to as BG.

3.2.1.2 Ultrasonication with surfactant coating (SG)

The pristine graphene (G) dispersion was conducted using a PC superplasticizer as a dispersant agent with the help of ultrasonication in a solution of water and a PC superplasticizer. The weight ratio of the PC superplasticizer to the graphene was equal to 9 to 1 as recommended by Papanikolaou et al. (2021) and verified by dynamic light scattering analysis (DLS) in this study. In order to fabricate graphene reinforced cement mortars, graphene aqueous suspensions were mixed with cement and sand following ASTM C109. The surfactant was first dissolved in water; after that, graphene was added to the solution. The resulting suspensions were then probe sonicated for 20 mins at an energy rate of 22-25 W, a frequency of 20 kHz, and an amplitude of 30% using an ultrasonic processor (Q700-QSonica LLC, 53 Church Hill Rd, Newtown, CT, USA). The total energy used was around 28000 J. The process of preparing graphene aqueous

solutions and the ultrasonication setup are shown in Figures (3.4) and (3.5). The cement mortar specimens cast by employing surfactant coating (PC) with the help of ultrasonication as the dispersion method of G, are herein referred to as SG.

3.2.2 Impact of graphene on the workability of cement mortars

Workability is a crucial parameter to assess the uniform mixing, placement, and compaction of cement mortars. The addition of supplementary materials such as nanomaterials will impact the workability of cement-based composite materials. Reduction of free water will occur as more water is needed to wet the large surface area of nanomaterials (Kumar et al., 2021). The workability of graphene reinforced cement mortar was measured using a flow test according to ASTM C 1437. The flow is the percentage increase in the average base diameter of the mortar mass with respect to the original base diameter. Two batches were tested on the flow table, shown in Figure (3.6), one was a control sample without the addition of graphene, and the other was with the addition of graphene by 0.04% BWOC. The mortar was placed in the flow mold in two layers. Each layer was about 25 mm and was tamped 20 times. After that, the flow table was dropped 25 times in 15 seconds as specified. Using the caliper specified in ASTM C 230, the four readings of the mortar diameter along the four lines scribed in the tabletop were added, and the total of those readings is the flow.

3.2.3 Dynamic Light Scattering (DLS) analysis

DLS analysis was used to assess the graphene aqueous suspensions. DLS analysis measures the average hydrodynamic radius (AHR) of particles in solutions. To compare the dispersion quality, the lesser the AHR values, the better the dispersion quality. Three surfactant/graphene weight ratios, namely 3:1, 6:1, and 9:1, were examined based on the

recommendation of Papanikolaou et al. (2021) and Islam et al. (2003). According to Islam et al. (2003), the optimum surfactant/CNT weight ratio was between 5 and 10 for different surfactant types. Moreover, Papanikolaou et al. (2021) used a polycarboxylate superplasticizer as a dispersant agent for graphene and reported that the 9:1 surfactant/graphene weight ratio significantly enhanced the graphene dispersion.

DLS analysis was employed using Zetasizer Pro, Malvern Panalytical. The DLS system was equipped with a high Avalanche Photodiode detector and a ten mW HeNe Laser at 633 nm wavelength. 1 mL samples of graphene aqueous suspension were examined in the DLS chamber. The samples were vortex-mixed before testing. Three measurements were collected at 30-second intervals for 15 minutes with the laser operating at whole exposure level and scattering data collected at 173° scattering angle. Each measurement was an average of 10 runs. The measurement with the lowest polydispersity index (PDI) was selected.

3.2.4 Scanning Electron Microscope (SEM) analysis

SEM analysis was used to study the microstructure of the cement-based composite samples. The samples were taken away from the fracture surfaces of the mortars. SEM images were taken using a Zeiss Gemini 500 Field Emission Scanning Electron Microscope (FESEM). The test samples were placed in a desiccator for several days then oven-dried at 60°C for 3 hours. The test samples were gold-sputtered before SEM examinations. Additionally, SEM analysis was used to show the morphology of the graphene powder used herein.

3.3 EXPERIMENTAL PROCEDURES

3.3.1 Fabrication of Specimens

3.3.1.1 Quantity of materials

Nine batches of cement mortar specimens were fabricated for the compressive strength test. Each batch consisted of six cubes with the dimensions of 50 mm by 50 mm by 50 mm. According to the suggestion of ASTM C 109, the water-cement ratio (w/c) was 0.485 for all the batches since this is the lowest w/c for mortar mixture without using a water-reducing agent. Moreover, based on the recommendation of ASTM C 109, the cement to sand ratio for all the batches was 1: 2.75 by weight. Graphene contents with 0.01%, 0.02%, 0.03%, and 0.04% by weight of cement (BWOC) were added to the cement mortars. The ratio of the PC superplasticizer to graphene was 9 to1, as recommended by Papanikolaou et al. (2021). The quantity of materials needed for each batch is shown in Table (3.4).

3.3.1.2 Casting of specimens

Procedures for casting the (CS) and (SG) specimens:

- 1- For the batches where graphene was added (SG), graphene suspensions with water and a dispersant agent (polycarboxylate superplasticizer) were prepared before mixing. Then, they were added to the mix as the mixing water for the (CS).
- 2- The mixing water, in the case of the (CS) batch, was placed in the bowl. (The graphene suspensions, in the case of the (SG) batches, were placed in the bowl.)
- 3- The cement was added to the water; then the mixer was started at a low speed of 140 rpm for 30 s.
- 4- The sand was added slowly over a 30 s period while mixing at a low speed.

- 5- The mixer was stopped, the speed was changed to a medium speed of 285 rpm, then the mixing continued for 30 s.
- 6- The mixer was stopped, and the mortar was left to stand for 90 s.
- 7- The mortar was mixed for 1 min at a medium speed of 285 rpm and poured into molds.
- 8- The mortar was placed into molds in two layers with proper tamping within a total elapsed time of 2 min and 30 s.

Procedures for casting (BG) specimens:

- 1- Cement, sand, mixing water, graphene, and dispersant agent (polycarboxylate superplasticizer) were placed in a bowl.
- 2- The mixture was stirred with a blender for 2 min at 300 rpm and poured into molds.
- 3- The mortar was placed into molds in two layers with proper tamping within a total elapsed time of 2 min and 30 s.

3.3.1.3 Curing of specimens

Immediately after completion of the molding, all test specimens were kept and covered with a plastic sheet for 24 hours. After that, they were immersed in saturated lime water in storage tanks until the time of testing.

3.3.2 Experimental setup

The compression strength test was performed on the 54 small cubes using a test frame of (MTS 810 Material Testing System, MTS systems Inc., Eden Prairie, Minnesota). The compression strength tests were performed under displacement control mode with a displacement rate of 0.01 mm/s. The load was applied to the specimen faces that were in contact with the plane surfaces of the mold. The test setup is shown in Figure (3.7).

3.4 REFERENCES

ASTM C109 / C109M-21, Standard Test Method for Compressive Strength of Hydraulic Cement Mortars (Using 2-in. or [50 mm] Cube Specimens), ASTM International, West Conshohocken, PA, 2021, www.astm.org

ASTM C1437-20, Standard Test Method for Flow of Hydraulic Cement Mortar, ASTM International, West Conshohocken, PA, 2020, www.astm.org

Islam, M. F., Rojas, E., Bergey, D. M., Johnson, A. T., & Yodh, A. G. (2003). High weight fraction surfactant solubilization of single-wall carbon nanotubes in water. *Nano letters*, 3(2), 269-273.

Li, G., Yuan, J. B., Zhang, Y. H., Zhang, N., & Liew, K. M. (2018). Microstructure and mechanical performance of graphene reinforced cementitious composites. *Composites Part A: Applied Science and Manufacturing*, 114, 188-195.

Papanikolaou, I., de Souza, L. R., Litina, C., & Al-Tabbaa, A. (2021). Investigation of the dispersion of multi-layer graphene nanoplatelets in cement composites using different superplasticiser treatments. *Construction and Building Materials*, 293, 123543.

3.5 TABLES

Table 3.1 Sieve analysis for sand

Sieve Number	Diameter (mm)	Weight Retained (g)	Percent Retained (%)	Cumulative Percent Retained (%)	Cumulative Percent passing (%)
4	4.75	0	0	0	100

10	2	0	0	0	100
20	0.85	187	13.6	13.6	86.4
30	0.6	627	45.6	59.2	40.7
40	0.425	432	31.4	90.6	9.3
50	0.3	97	7	97.7	2.3
100	0.15	29	2.1	99.8	0.2
				$\Sigma=361$	

Table 3.2 Physical and chemical properties of pristine graphene

Type of graphene	Appearance	Physical state	Solubility (water)	Average particle size (μm)	Thickness (nm)	Purity
ProCene Graphene	Black	Solid	Negligible	12	0.3-10	99 wt.*%

*By weight of carbon

Table 3.3 Properties of Superplasticizer

Superplasticizer Type	Appearance	Physical state	Solid content (%)	Specific Gravity
Polycarboxylate Polymer	Blue	Liquid	35	1.08

Table 3.4 Quantity of materials for compression test

Batch	Number of Specimens	% Of graphene (BWOC)	Weight of Cement (g)	Weight of Sand (g)	Weight of Water (mL)	Weight of Graphene (mg)	Weight of PC (mg)
CS	6	0	500	1375	242	0	0
SG 1	6	0.01	500	1375	242	50	450
SG 2	6	0.02	500	1375	242	100	900
SG 3	6	0.03	500	1375	242	150	1350
SG 4	6	0.04	500	1375	242	200	1800
BG 1	6	0.01	500	1375	242	50	450
BG 2	6	0.02	500	1375	242	100	900

BG 3	6	0.03	500	1375	242	150	1350
BG 4	6	0.04	500	1375	242	200	1800

*CS is the control batch (reference) with no addition of graphene

*(S or B) refer to the method used for graphene dispersion, (S) for the ultrasonication, and (B) for the mechanical blending.

* G refers to the addition of graphene.

3.6 FIGURES

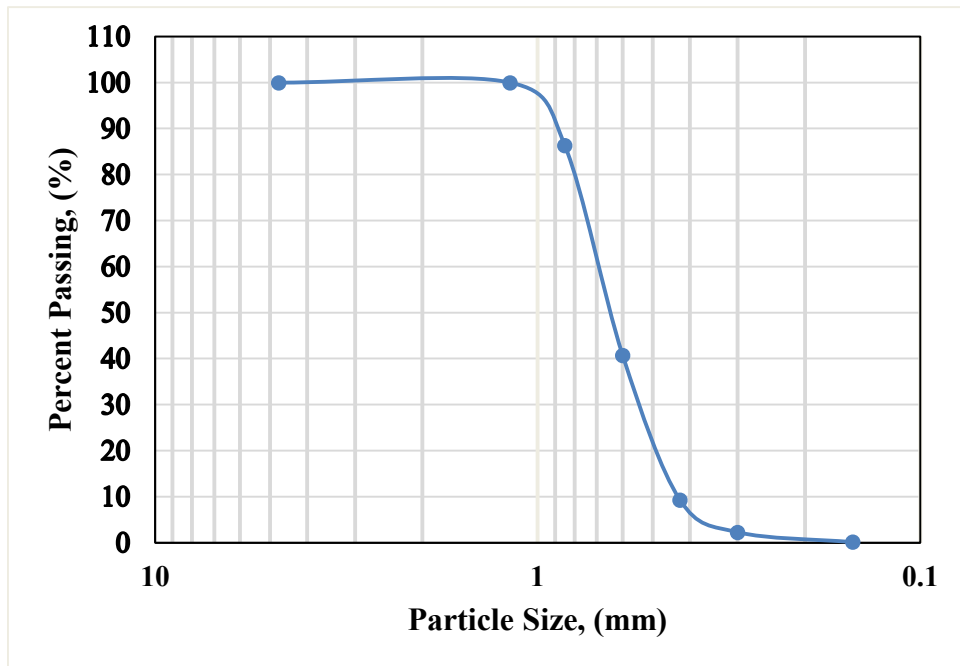


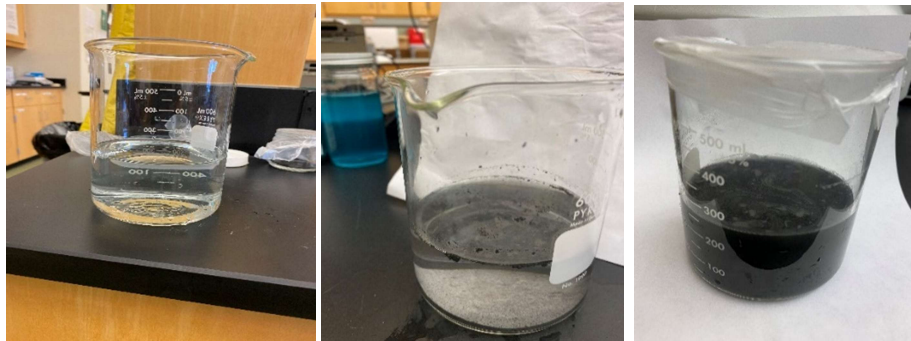
Figure 3.1 Particle size distribution curve for sand



Figure 3.3 As received graphene powder



Figure 3.2 Sika-ViscoCrete 2100 (polycarboxylate superplasticizer)



water + Sika Viscocrete 2100 (PC)

Before Sonication:
Graphene + water +
Sika Viscocrete 2100
(PC)

Graphene aqueous
suspensions after
sonication

Figure 3.4 The process of preparation of graphene aqueous suspensions

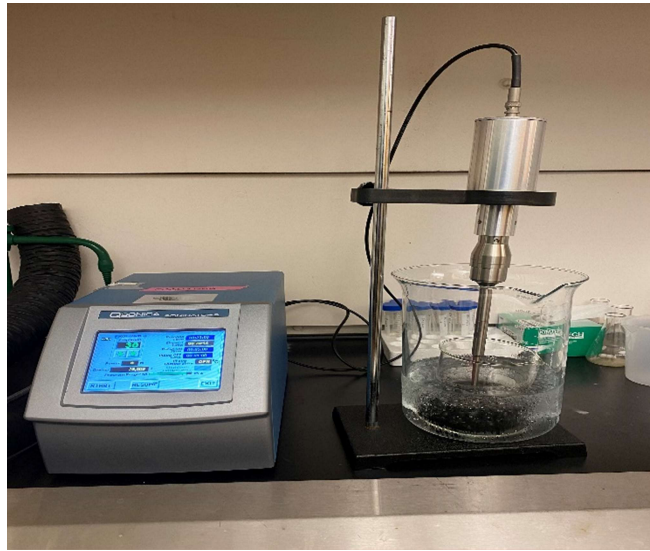


Figure 3.5 Ultrasonication Setup



Figure 3.6 Flow Table

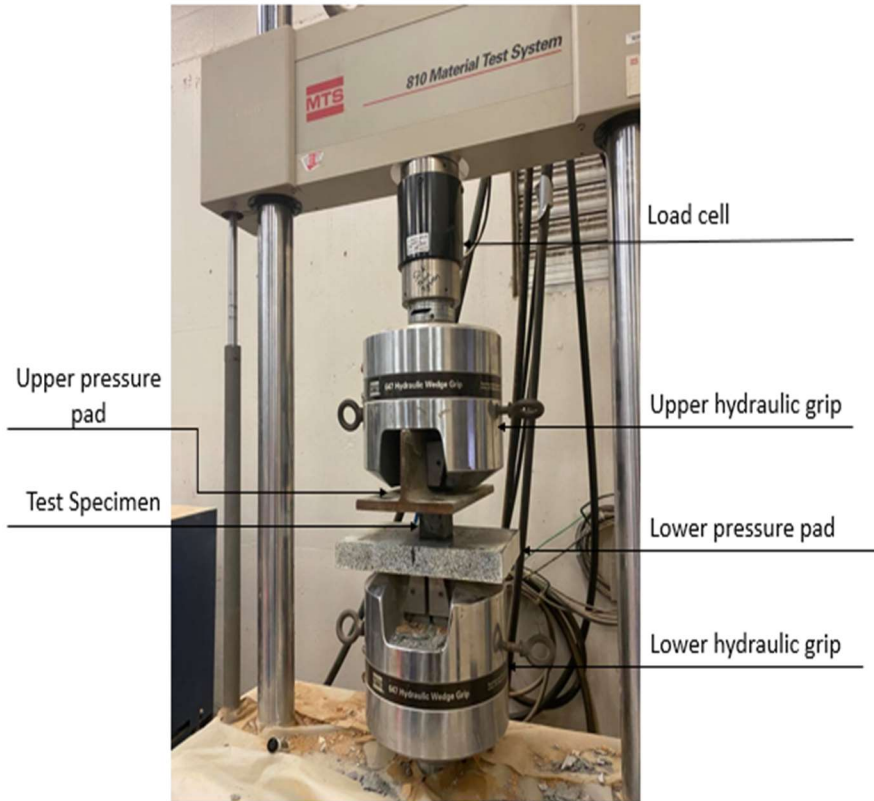


Figure 3.7 Compression Test Setup

CHAPTER 4

RESULTS AND DISCUSSIONS

4.1 INTRODUCTION

In this chapter the results of the investigation to discover the impact of adding pristine graphene on the workability of plain cement mortars and graphene reinforced cement mortars are discussed. The suitable surfactant (PC) to graphene (G) weight ratio was chosen based on the comparison between the AHR values for graphene aqueous suspensions with different surfactant concentrations employing DLS analysis. Moreover, DLS analysis was used to assess the effect of ultrasonication on graphene aqueous suspensions. The selected surfactant to graphene weight ratio was used to fabricate the G reinforced mortar cubes. The compression test results are discussed, and stress-strain curves for the tests are shown. SG reinforced cement mortars results were compared to BG reinforced cement mortars, which showed small differences between the ultrasonication with surfactant coating dispersion technique and the mechanical blending with surfactant coating. Hence, the mechanical blending with surfactant coating was a more convenient method in terms of practicality and easiness to be applied for large scale applications. Finally, an assessment of the impact of the addition of graphene to the microstructure of cement mortars and to justify the increase in the compressive strength is explained. SEM micrographs for the microstructure of plain cement mortars and graphene reinforced cement mortars are shown.

4.2 WORKABILITY OF CEMENT MORTARS

Figure (4.1) presents the flow test results of the flow measurements of graphene reinforced cement mortars for workability study. The flow values for 0% and 0.04% (BWOC) graphene reinforced cement mortars were 119% and 120%, respectively. The addition of graphene at these low concentrations did not affect the workability of the cement mortars. The impact on the workability of cement-based composite materials reinforced with pristine graphene documented herein agrees with the findings of Qureshi and Panesar (2020). They measured the static and dynamic flows using a mini-slump test. They reported that pristine graphene incorporated in cement pastes at low concentrations-.01, 0.02, 0.04, 0.08, and 0.16% by weight of cement- did not impact the workability of the cement paste since pristine graphene is hydrophobic. However, incorporating functionalized graphene (GO) with the same concentrations decreased the workability of cement pastes. The static and dynamic flows for the 0.16% by weight of cement GO cement paste was approximately 28% and 11% less than the control mix due to the presence of the hydrophilic functional groups on the surface of GO.

4.3 OPTIMUM SURFACTANT TO GRAPHENE WEIGHT RATIO

The AHR values resulting from the DLS analysis on the graphene aqueous suspensions with different surfactant/graphene weight ratios are presented in Figure (4.2). In order to compare the dispersion quality, the highest quality of dispersion is indicated by the minimum AHR value. The AHR values were 309.6 nm, 345.5 nm, and 409.3 nm for 9 to 1, 6 to 1, and 3 to 1 surfactant/graphene weight ratio. The corresponding PDI index values were 0.494, 0.465, and 0.539 for 9 to 1, 6 to 1, and 3 to 1 surfactant/graphene weight ratio, respectively. Based on the results as shown in Figure (4.1), a surfactant to graphene

weight ratio of 9 to 1 was adopted in this study. The results agree with the findings of Papanikolaou et al. (2021) and Islam et al. (2003).

4.4 DLS ANALYSIS OF GRAPHENE AQUEOUS SUSPENSIONS

Figure (4.3) presents the effect of the surfactant coating with the aid of ultrasonication on the dispersion of graphene materials based on the AHR values of the graphene aqueous suspensions before and after ultrasonication at surfactant to graphene ratio 9 to 1. The AHR value of graphene aqueous suspensions before the application of the ultrasonication was 1416 nm with a corresponding PDI value of 0.592, while after sonication, the AHR value was 309.6 nm with a corresponding PDI value of 0.494. The results showing the importance of ultrasonication in creating a better dispersion for the graphene aqueous solutions.

4.5 COMPRESSIVE STRENGTH

The impact of incorporating graphene with different concentrations and different dispersion techniques on the compressive strength of cement mortar was investigated by a compression strength test according to ASTM C 109. The compression test results for all specimens of different batches are shown in Table (A.1). Additionally, a comparison between the average compressive strength for each batch is shown in Figure (4.4) and Table (4.1). The error bars shown in Figure (4.4) represent the standard deviation, which measures the variability of the specimens of each batch.

The acquired improvement in the compressive strength of graphene reinforced cement mortars compared to plain cement mortars, as shown in Figure (4.4), can be attributed to a set of distinct reasons as reported in the literature. First, the incorporation of

graphene into cement-based composite materials enhanced the number of hydration products, which filled cracks and holes (Wang and Zhao, 2018 and Qureshi and Panesar, 2020). Second, graphene acted as nucleation sites for C-S-H gel, which precipitated around the graphene, creating a denser microstructure (Tong et al., 2015). Third, the addition of graphene reduced the porosity and pore sizes of cement-based composite materials (Wang and Zhao, 2018). However, at higher dosages (0.04% BWOC) of G, the graphene sheets agglomerated, reducing the beneficial effect of adding graphene (Li et al., 2018).

4.6.1 Mechanical Blending with surfactant coating (BG)

Four batches, BG1, BG2, BG3, and BG4, reinforced mortar cubes, were tested to determine the compressive strength. The average compressive strength was 36.9 ± 1.7 MPa, 40.5 ± 1.3 MPa, 42.3 ± 2.4 MPa, and 39.7 ± 1.6 MPa for BG1, BG2, BG3, and BG4 reinforced mortar cubes. The incorporation of graphene resulted in an increase in the average compressive strength for BG1, BG2, BG3, and BG4 by 16.4%, 27.9%, 33.6%, and 25.6%, respectively, compared to the control specimens (CS). That increase in the compressive strength of BG reinforced cement mortars batches compared to the control specimens verified the excellent quality of the dispersion method employed. However, this is an indirect measure of the dispersion of G. The stress-strain curves for each batch are presented in Figures (4.5), (4.6), (4.7), and (4.8).

4.6.2 Ultrasonication with surfactant coating (SG)

Four batches, SG1, SG2, SG3, and SG4, of reinforced mortar cubes, were tested to determine their compressive strength. The average compressive strength was 37.0 ± 1.4 MPa, 41.9 ± 2.5 MPa, 43.7 ± 1.9 MPa, and 38.8 ± 2.2 MPa for SG1, SG2, SG3, and SG4 reinforced mortar cubes, respectively. The incorporation of graphene employing

ultrasonication with the help of surfactant coating (PC) as a dispersion method resulted in an increase in the average compressive strength for SG1, SG2, SG3, and SG4 by 17.0%, 32.4%, 38.0, and 22.5%, respectively, compared to the control specimens (CS). That increase in the compressive strength of SG reinforced cement mortars batches compared to the control specimens verified the excellent quality of the dispersion method employed. Also, for the exact graphene dosage, SG batches showed more of an increase in compressive strength compared to BG batches, which indicates the superiority of the dispersion method employed for casting SG batches than BG batches. The stress-strain curves for each batch are presented in Figures (4.9), (4.10), (4.11), and (4.12).

Figure (4.13) presents a comparison between the two dispersion methods employed herein in this study at each dosage of G. The average compressive strength, together with the error bars showing the standard deviation, is shown for the graphene reinforced cement mortars batches fabricated. The results illustrate that the two-dispersion method had a very similar outcome on the mechanical performance of cement mortars. However, mechanical blending with surfactant coating was a more convenient method in terms of practicality and easiness than ultrasonication with surfactant coating. Applying ultrasonication will be an obstacle to preparing graphene aqueous suspensions for large-scale applications in industry.

4.6 MICROSTRUCTURE OF CEMENT MORTARS

SEM was used to assess the morphology of the as-received graphene powder and the microstructure of the cement mortars. Figures (4.14) and (4.15) show the morphology of as-received graphene powder. In addition, the graphene sheets were about 10 μm width and 30 μm length, which agree with the findings of (Li et al., 2018). The graphene sheets

appeared to be translucent, with wrinkles texture on their surface and randomly aggregated.

The increase in compressive strength reported herein can be justified by SEM micrographs. The addition of graphene enhanced the amount of the hydration products which filled cracks. Thus, the microstructure of plain cement mortar around a crack is presented in Figure (4.16). On the other hand, the microstructure of graphene reinforced cement mortar (0.02% of G) is presented in Figures (4.17). Figure (4.18) and (4.19) show hydration products forming a structure together. It is possible that the hydration products precipitated around graphene, as graphene acts as nucleation sites for the hydration products. At higher dosages (0.04% BWOC) of G, the graphene sheets agglomerated, reducing the beneficial effect of adding graphene as presented in Figure (4.20).

4.7 COST ANALYSIS

Table (4.2) presents the cost analysis of the materials used in fabricating the cement mortars batches. The total cost was calculated for the materials required per cubic meter. A comparison of the total cost for each batch is shown in Table (4.2). It can be observed that the mechanical blending with surfactant coating (BG) dispersion method is cheaper than the ultrasonication with surfactant coating (SG). The percent increase in the cost for BG batches was 38%, 76%, 114%, and 152% for BG1, BG2, BG3, and BG4, respectively, compared to the control batch. On the other hand, for SG batches, the increase was 287%, 325%, 363%, and 401%, respectively. The cost of the materials as provided by the suppliers is presented in Table (A.2).

4.8 TABLES

Table 4.1 Average Compressive Strength for mortar batches

Batch	Graphene dosage (%)	28-day Average Compressive strength \pm Standard deviation (MPa)	Increase (%)
CS	0	31.6 \pm 1.6	N/A
SG1	0.01	37.0 \pm 1.4	17.0
SG2	0.02	41.9 \pm 2.5	32.4
SG3	0.03	43.7 \pm 1.9	38.0
SG4	0.04	38.8 \pm 2.2	22.5
BG1	0.01	36.9 \pm 1.7	16.4
BG2	0.02	40.5 \pm 1.3	27.9
BG3	0.03	42.3 \pm 2.4	33.6
BG4	0.04	39.7 \pm 1.6	25.6

* CS is the control batch (reference) with no addition of graphene

*(S or B) refer to the method used for graphene dispersion, (S) for the ultrasonication, and (B) for the mechanical blending.

* G refers to the addition of graphene

* N/A refers to not applicable

Table 4.2 Cost analysis for mortar batches

Batch	Mass of materials (kg) per m ³				Ultrasonication Cost (\$/m ³)	Total Cost (\$/m ³)	Increase (%)
	cement	sand	G	PC			
CS	667	1833	0	0	0	892.8	N/A
SG1	667	1833	0.07	0.6	2222	3454.2	287
SG2	667	1833	0.13	1.2	2222	3793.5	325
SG3	667	1833	0.20	1.8	2222	4132.8	363
SG4	667	1833	0.27	2.4	2222	4472.2	401
BG1	667	1833	0.07	0.6	0	1232.2	38
BG2	667	1833	0.13	1.2	0	1571.5	76
BG3	667	1833	0.20	1.8	0	1910.8	114

BG4	667	1833	0.27	2.4	0	2250.2	152
-----	-----	------	------	-----	---	--------	-----

* CS is the control batch (reference) with no addition of graphene

*(S or B) refer to the method used for graphene dispersion, (S) for the ultrasonication, and (B) for the mechanical blending.

* G refers to the addition of graphene

* N/A refers to not applicable

4.9 FIGURES

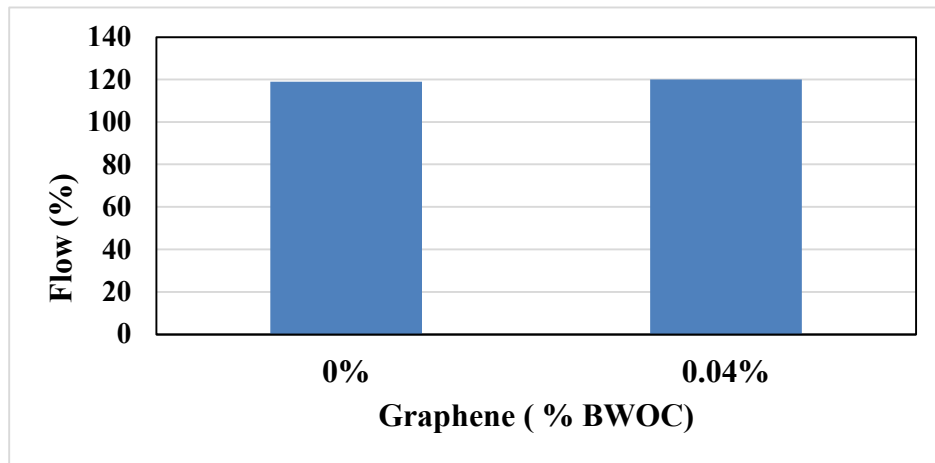


Figure 4.1 Flow of cement mortars with 0% and 0.04% graphene BWOC

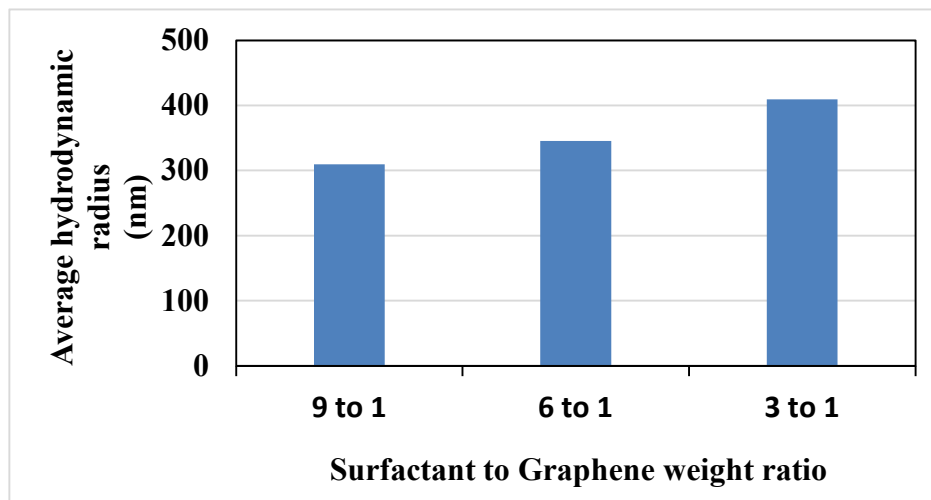


Figure 4.2 AHR values of graphene suspensions with a different surfactant ratio

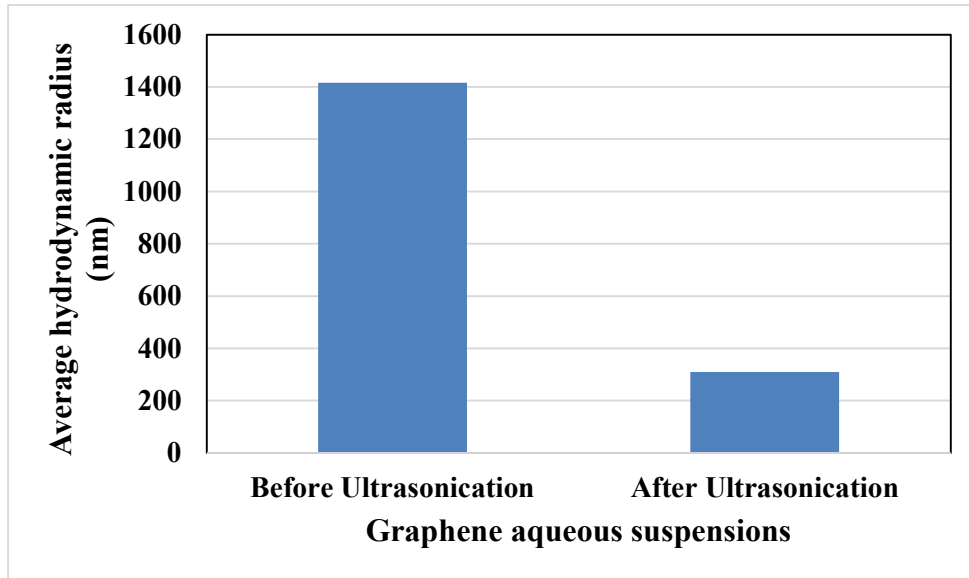


Figure 4.3 AHR values of graphene suspensions before and after ultrasonication

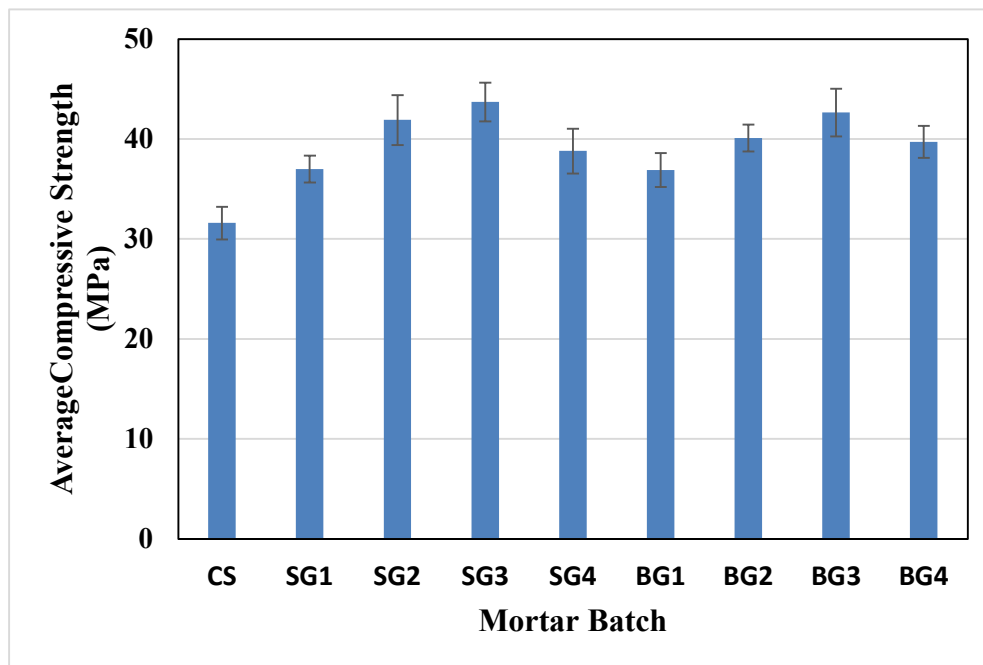


Figure 4.4 Average compressive strength of the mortar batches tested

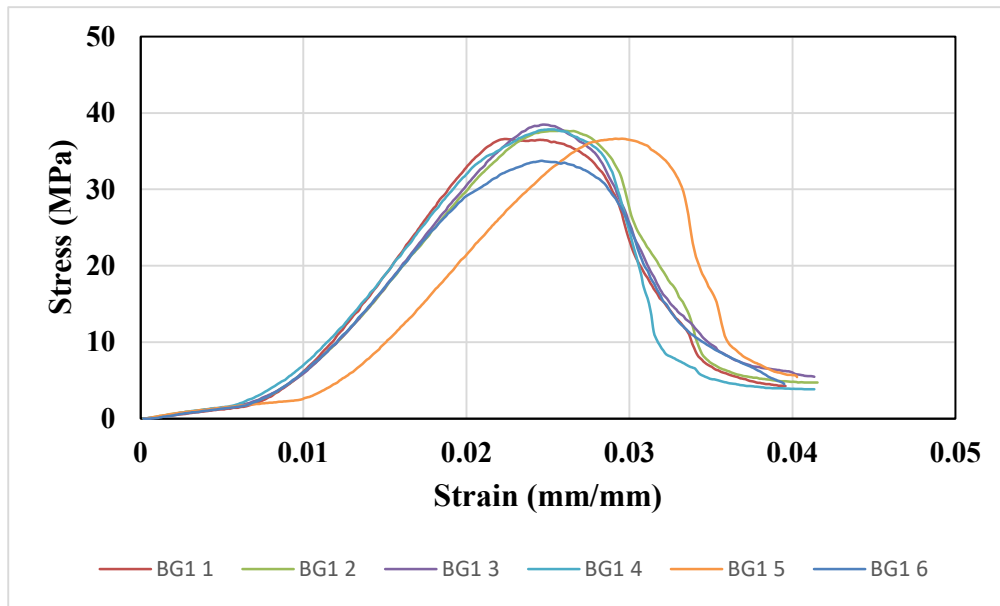


Figure 4.5 Stress-Strain curves for BG1 reinforced mortar cubes

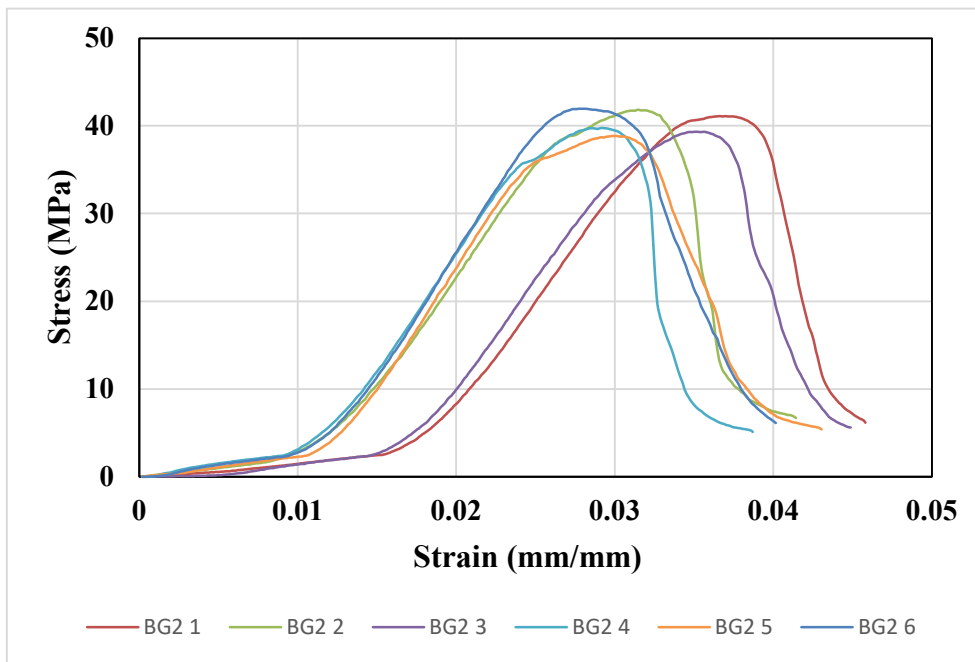


Figure 4.6 Stress-Strain curves for BG2 reinforced mortar cubes

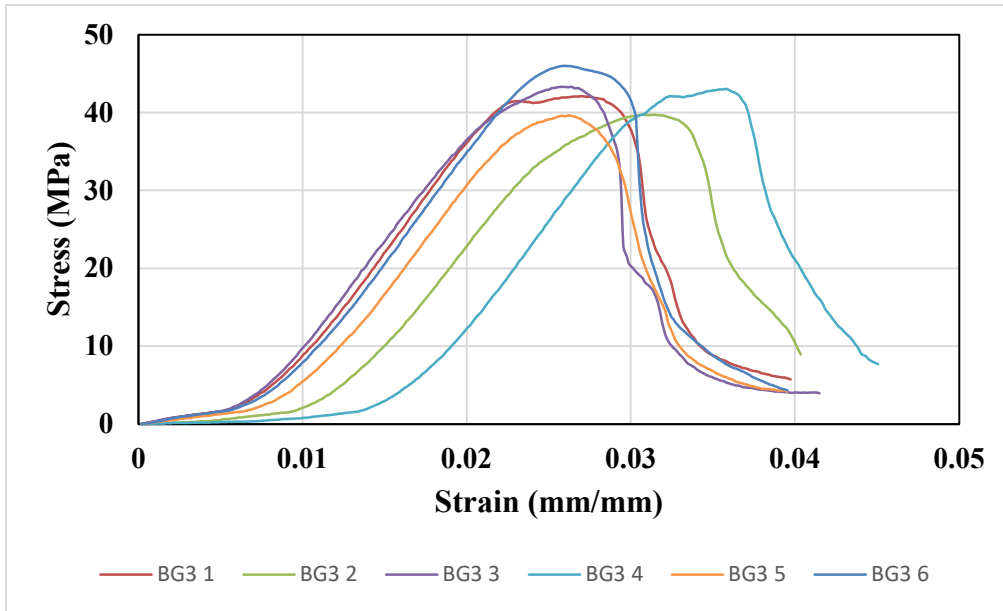


Figure 4.7 Stress-Strain curves for BG3 reinforced mortar cubes

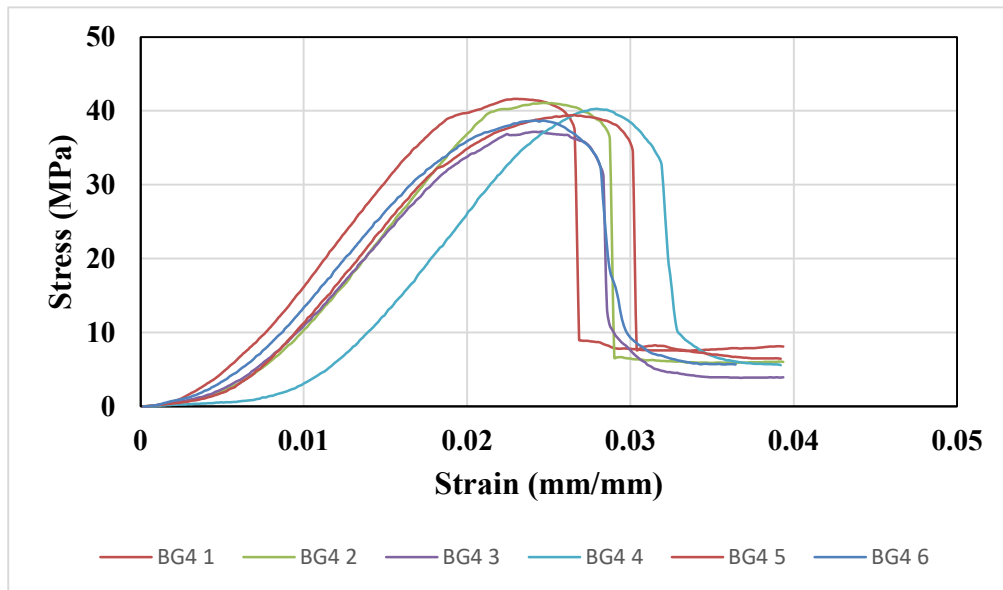


Figure 4.8 Stress-Strain curves for BG4 reinforced mortar cubes

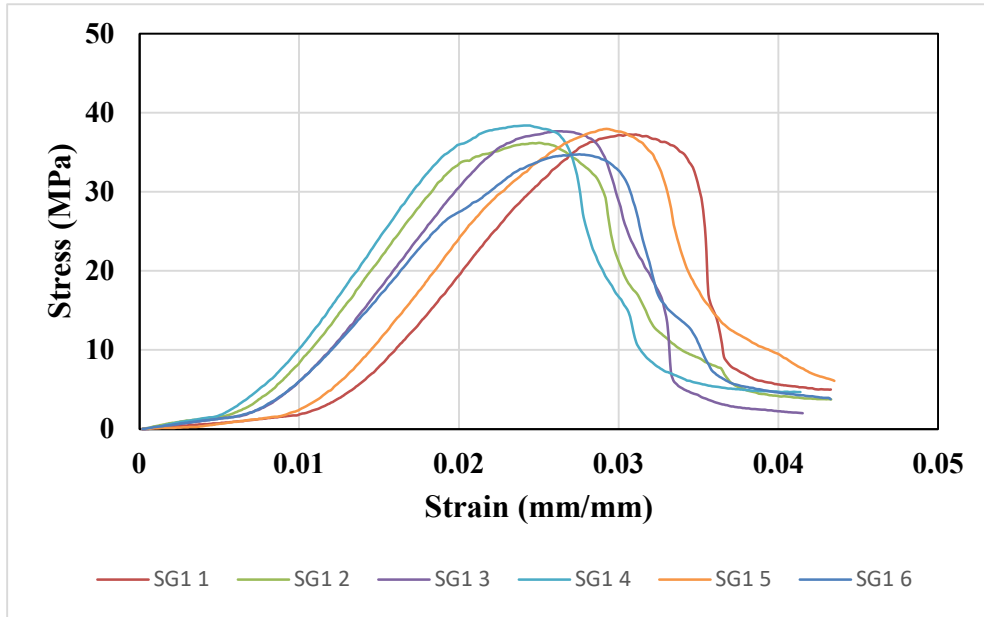


Figure 4.9 Stress-Strain curves for SG1 reinforced mortar cubes

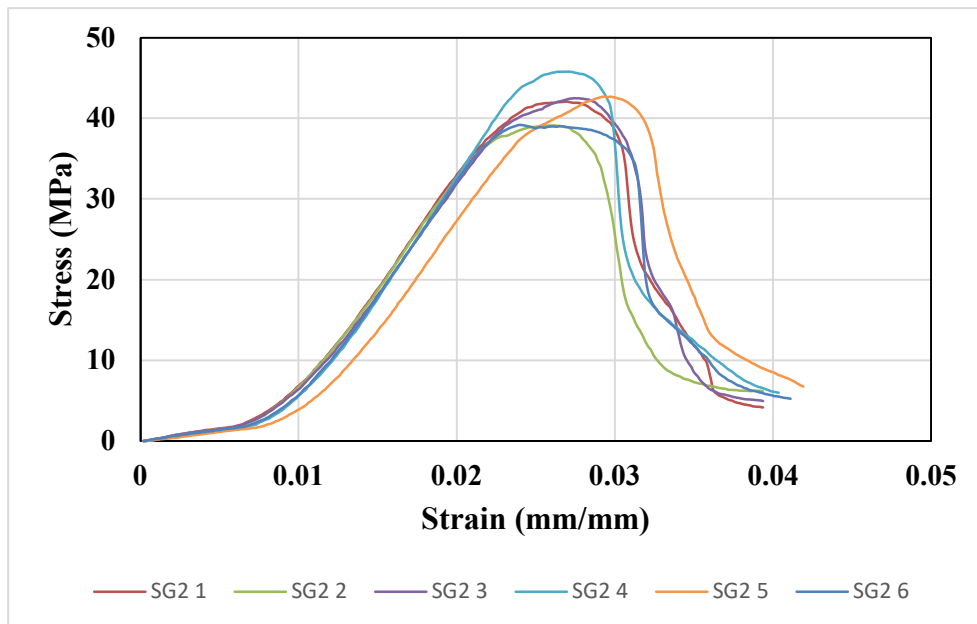


Figure 4.10 Stress-Strain curves for SG2 reinforced mortar cubes

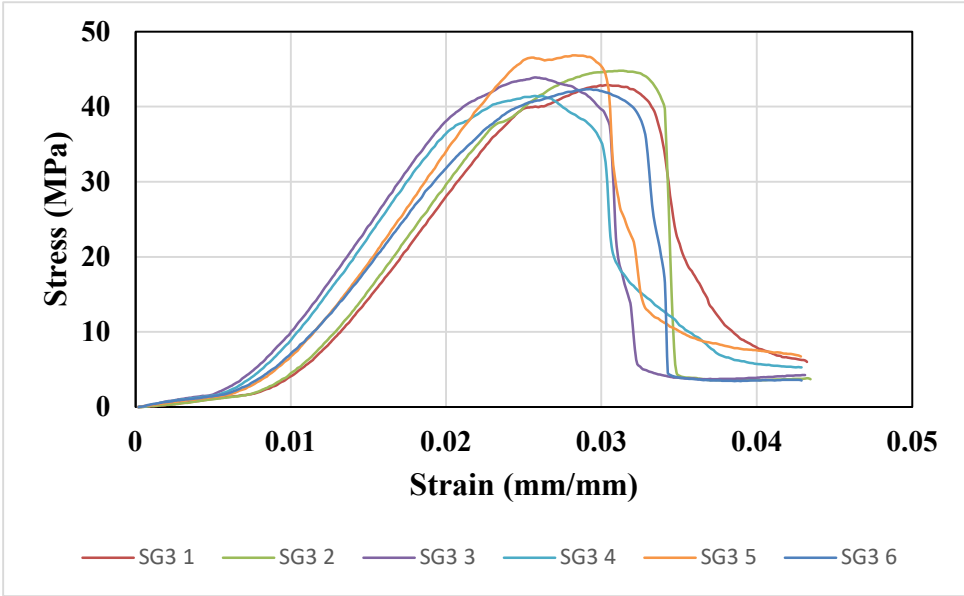


Figure 4.11 Stress-Strain curves for SG3 reinforced mortar cubes

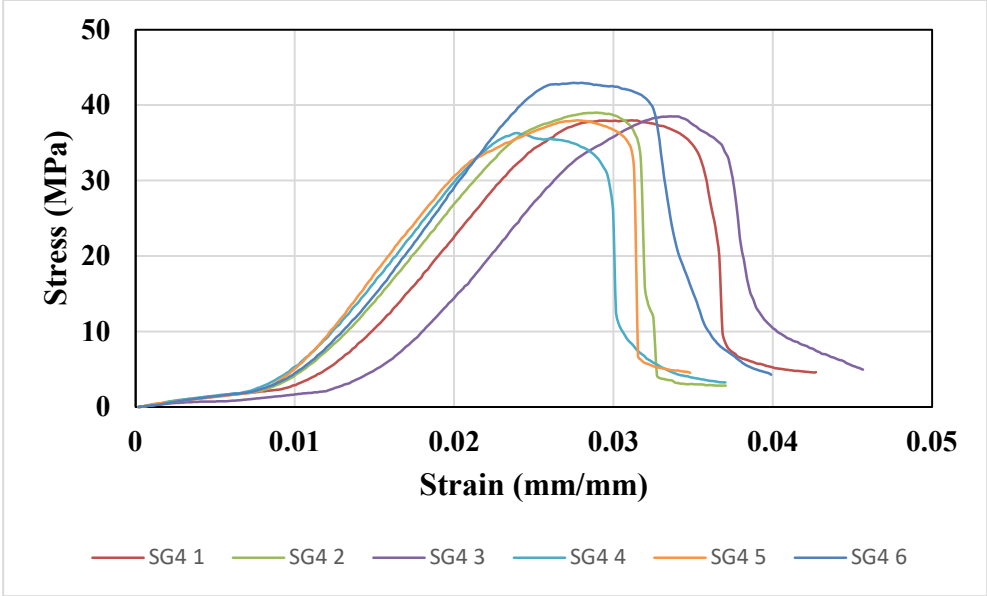


Figure 4.12 Stress-Strain curves for SG4 reinforced mortar cubes

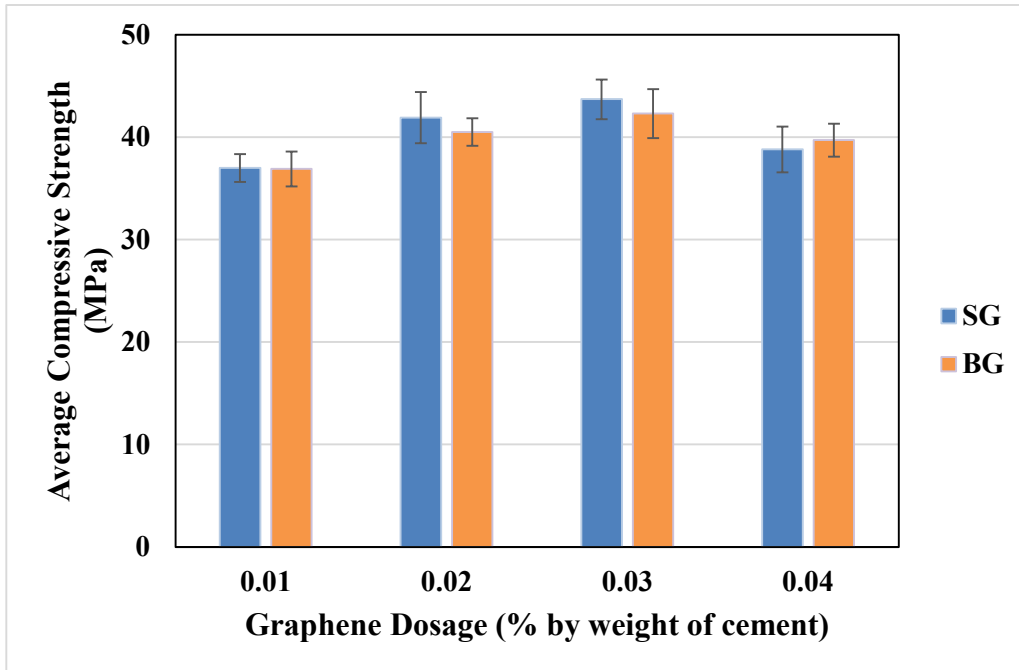


Figure 4.13 Comparison between the dispersion methods at each graphene dosage.

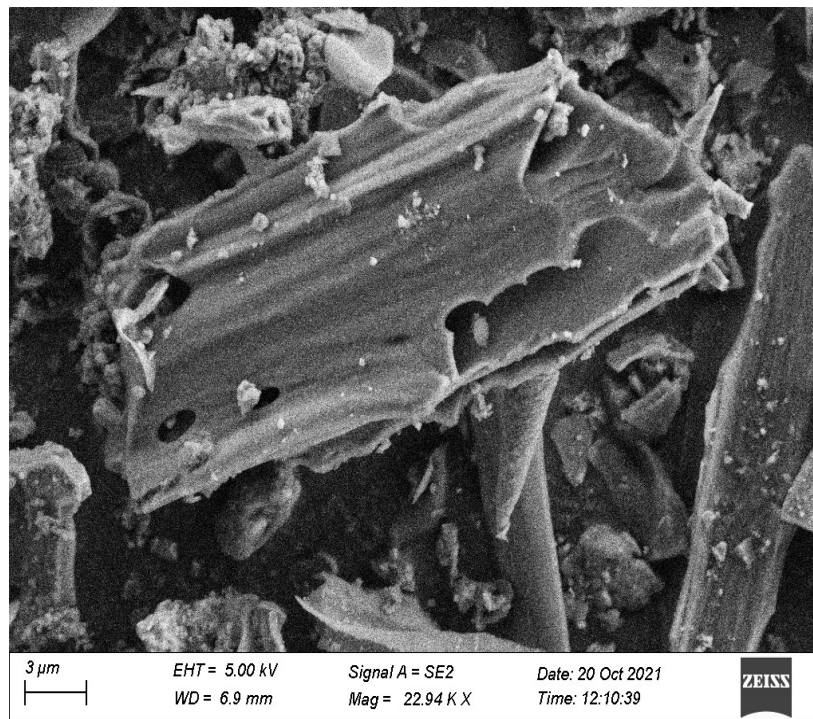


Figure 4.14 SEM micrograph of as-received graphene powder

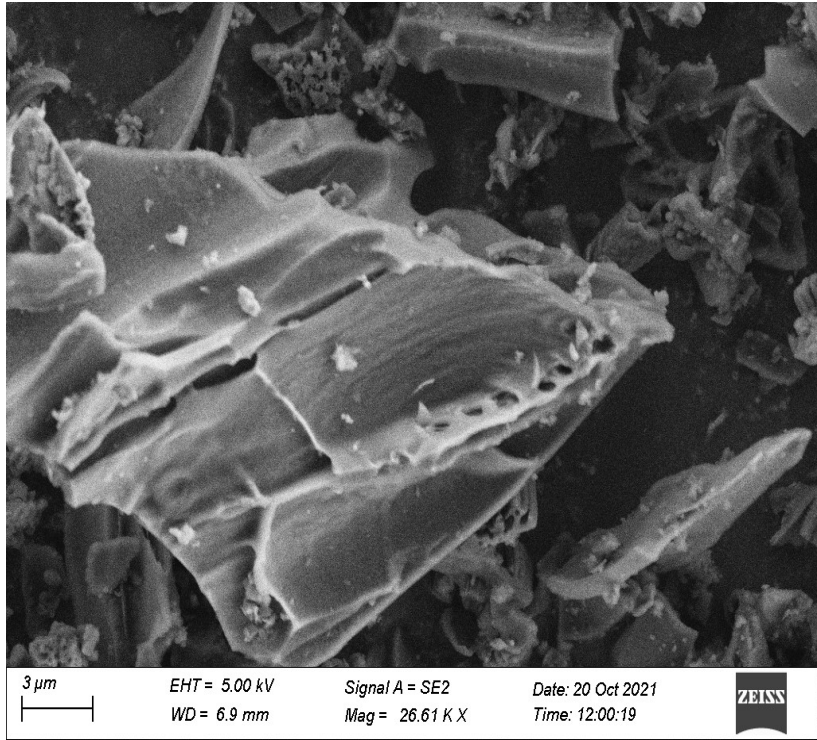


Figure 4.15 SEM micrograph showing the aggregation of as-received graphene

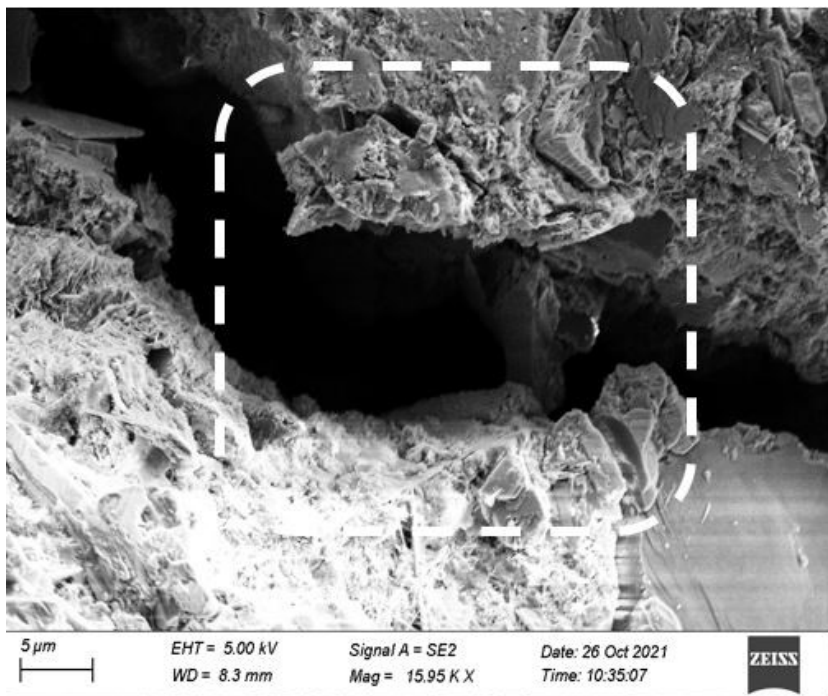


Figure 4. 16 Microstructure of plain cement mortar

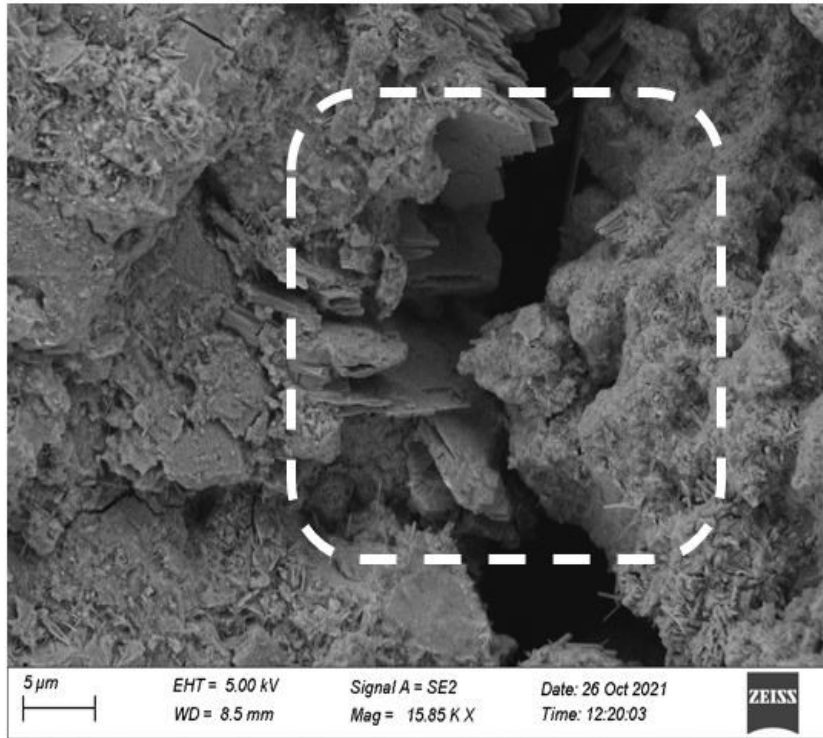


Figure 4.17 Microstructure of mortar mix containing 0.02% graphene

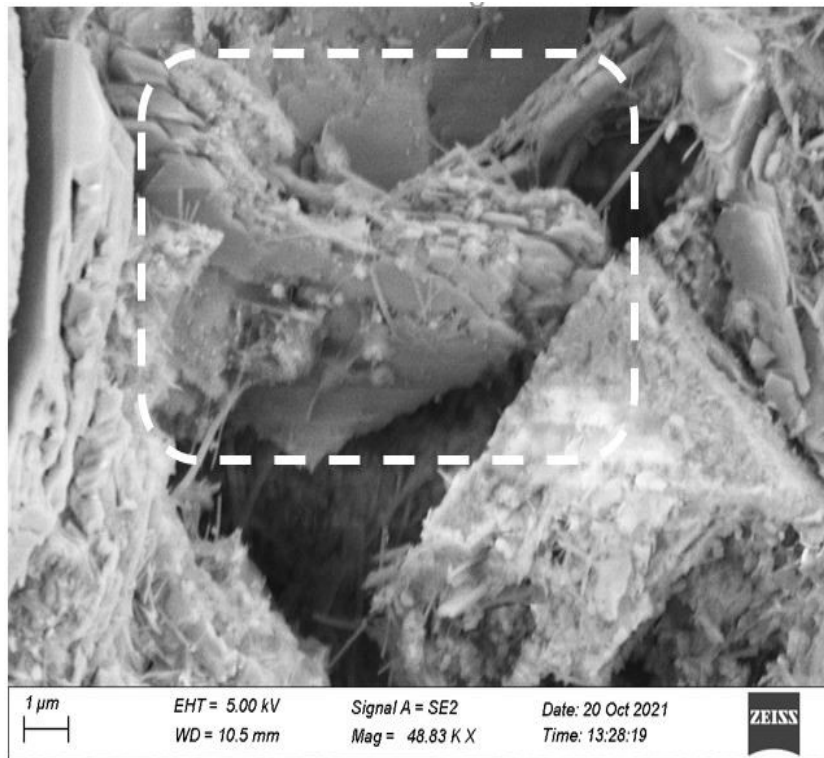


Figure 4.18 Microstructure of mortar mix containing 0.03% graphene

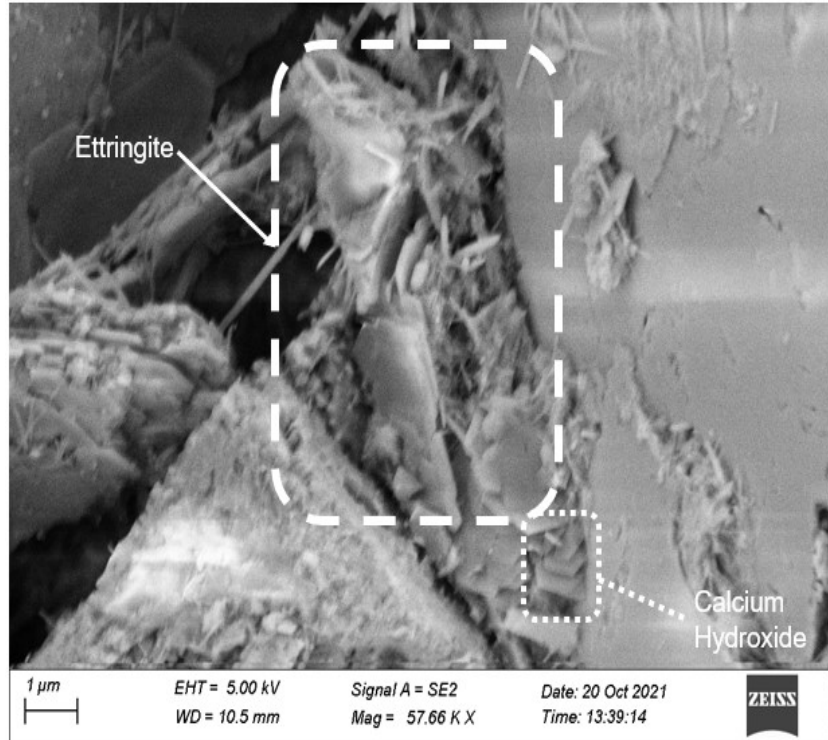


Figure 4.19 Hydration products in mortar mix containing 0.03% graphene

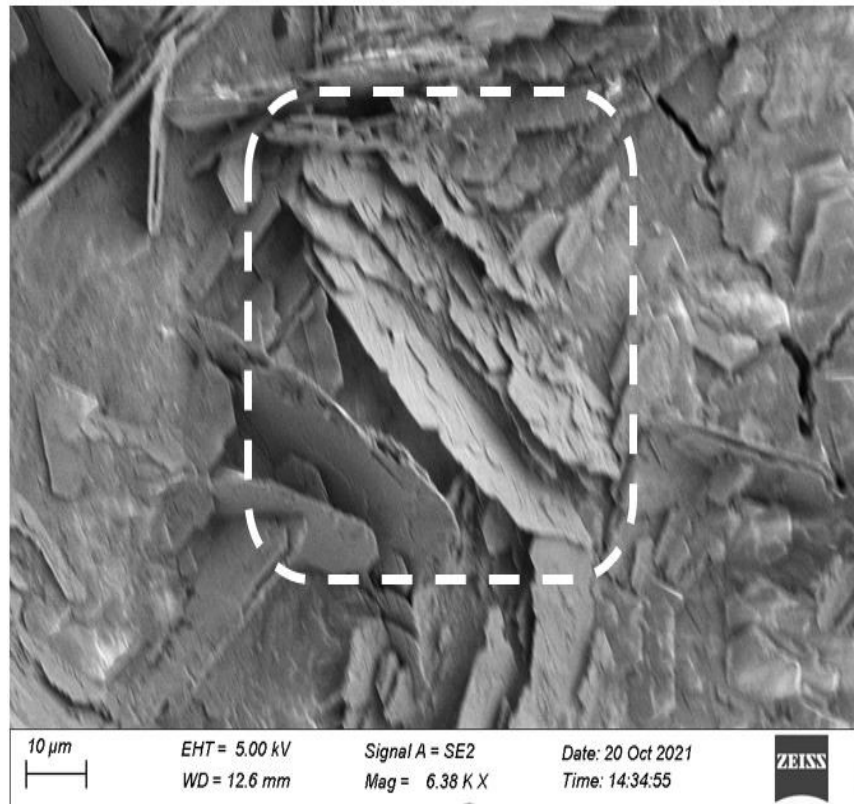


Figure 4.20 Agglomeration of graphene sheets in mortar mix at 0.04% concentration

CHAPTER 5

SUMMARY AND CONCLUSIONS

5.1 SUMMARY AND CONCLUSIONS

This study aimed to determine the impact of the addition of G in low dosages (%-BWOC) on the compressive strength of the cement mortars and to compare between two different dispersion methods for G in cement mortars, which are mechanical blending with surfactant coating and ultrasonication with surfactant coating. A polycarboxylate superplasticizer (Sika Viscocrete 2100) was used as a dispersant agent (surfactant) of graphene. The conclusions of this study are:

- The addition of pristine graphene at this low dosage (0.04%) by weight of cement did not impact the workability of cement mortars.
- The addition of pristine graphene up to 0.03% by weight of cement enhances the mechanical properties of cement mortars. At higher dosages, the graphene agglomerates which leads to a decrease in the beneficial impact of adding pristine graphene. At 0.03% by weight of cement for the mechanical blending with surfactant coating method, the increase in compressive strength was 33.6%, while at 0.04% by weight of cement, the increase was 22.5%. Additionally, at 0.03% by weight of cement for the ultrasonication with surfactant coating method, the

increase in compressive strength was 38%, while at 0.04% by weight of cement, the increase was 25.6%.

- Two different dispersion methods for pristine graphene in cement mortars were investigated to understand their effect on the mechanical properties, which resulted in very similar outcomes. Yet, the mechanical blending with surfactant coating was a more convenient method than ultrasonication with surfactant coating in terms of practicality, easiness, and cost to be applied in industry for large scale applications.

5.2 RECOMMENDATIONS FOR FUTURE WORK

This section indicates more investigations to be carried out for future work:

- Effect of graphene reinforcement on porosity reduction and cement hydration: the incorporation of graphene as a nanoreinforcement in cement based composite materials was reported to reduce the porosity and promote the formation of denser cement hydrates. Further research is needed to address the underlying mechanisms.
- Effect of w/c ratio: the impact of the w/c ratio on the mechanical performance of the graphene reinforced cement based composite materials. Further research is needed to understand the relationship between the w/c and the mechanical properties of graphene reinforced cement composites.
- Effect of adding graphene reinforcement to concrete: most of the studies carried out reported the effect of the addition of graphene and its derivatives on the mechanical and transport properties of cement paste. Hence, more studies will need to be carried out on the addition of graphene and its derivatives to concrete from both the material and structural perspectives.

REFERENCES

- Anagnostopoulos, C. A. (2014). Effect of different superplasticisers on the physical and mechanical properties of cement grouts. *Construction and Building Materials*, *50*, 162-168.
- Balandin, A. A., Ghosh, S., Bao, W., Calizo, I., Teweldebrhan, D., Miao, F., & Lau, C. N. (2008). Superior thermal conductivity of single-layer graphene. *Nano letters*, *8*(3), 902-907.
- Baquerizo, L. G., Matschei, T., Scrivener, K. L., Saeidpour, M., & Wadsö, L. (2015). Hydration states of AFm cement phases. *Cement and Concrete Research*, *73*, 143-157.
- Bolotin, K. I., Sikes, K. J., Jiang, Z., Klima, M., Fudenberg, G., Hone, J., ... & Stormer, H. L. (2008). Ultrahigh electron mobility in suspended graphene. *Solid state communications*, *146*(9-10), 351-355.
- Cao, M., Zhang, C., & Wei, J. (2013). Microscopic reinforcement for cement based composite materials. *Construction and Building Materials*, *40*, 14-25.
- Chakraborty, S., Kundu, S. P., Roy, A., Adhikari, B., & Majumder, S. B. (2013). Effect of jute as fiber reinforcement controlling the hydration characteristics of cement matrix. *Industrial & Engineering Chemistry Research*, *52*(3), 1252-1260.

- Chuah, S., Pan, Z., Sanjayan, J. G., Wang, C. M., & Duan, W. H. (2014). Nano reinforced cement and concrete composites and new perspective from graphene oxide. *Construction and Building Materials*, 73, 113-124.
- Dalla, P. T., Tragazikis, I. K., Trakakis, G., Galiotis, C., Dassios, K. G., & Matikas, T. E. (2021). Multifunctional Cement Mortars Enhanced with Graphene Nanoplatelets and Carbon Nanotubes. *Sensors*, 21(3), 933.
- Dikin, D. A., Stankovich, S., Zimney, E. J., Piner, R. D., Dommett, G. H., Evmenenko, G., ... & Ruoff, R. S. (2007). Preparation and characterization of graphene oxide paper. *Nature*, 448(7152), 457-460.
- Du, H., & Dai Pang, S. (2015). Enhancement of barrier properties of cement mortar with graphene nanoplatelet. *Cement and Concrete Research*, 76, 10-19.
- Holschemacher, K., Mueller, T., & Ribakov, Y. (2010). Effect of steel fibres on mechanical properties of high-strength concrete. *Materials & Design (1980-2015)*, 31(5), 2604-2615.
- Holschemacher, K., Mueller, T., & Ribakov, Y. (2010). Effect of steel fibres on mechanical properties of high-strength concrete. *Materials & Design (1980-2015)*, 31(5), 2604-2615.
- Hu, J., Ge, Z., & Wang, K. (2014). Influence of cement fineness and water-to-cement ratio on mortar early-age heat of hydration and set times. *Construction and building materials*, 50, 657-663.

- Indukuri, C. S. R., & Nerella, R. (2021). Enhanced transport properties of graphene oxide-based cement composite material. *Journal of Building Engineering*, 37, 102174.
- Islam, M. F., Rojas, E., Bergey, D. M., Johnson, A. T., & Yodh, A. G. (2003). High weight fraction surfactant solubilization of single-wall carbon nanotubes in water. *Nano letters*, 3(2), 269-273.
- Jing, G., Ye, Z., Lu, X., & Hou, P. (2017). Effect of graphene nanoplatelets on hydration behaviour of Portland cement by thermal analysis. *Advances in Cement Research*, 29(2), 63-70.
- Lee, C., Wei, X., Kysar, J. W., & Hone, J. (2008). Measurement of the elastic properties and intrinsic strength of monolayer graphene. *science*, 321(5887), 385-388.
- Li, G., Yuan, J. B., Zhang, Y. H., Zhang, N., & Liew, K. M. (2018). Microstructure and mechanical performance of graphene reinforced cementitious composites. *Composites Part A: Applied Science and Manufacturing*, 114, 188-195.
- Li, H., Xiao, H. G., Yuan, J., & Ou, J. (2004). Microstructure of cement mortar with nanoparticles. *Composite's part B: engineering*, 35(2), 185-189.
- Lin, Y., & Du, H. (2020). Graphene reinforced cement composites: A review. *Construction and Building Materials*, 265, 120312.
- Lv, S., Liu, J., Sun, T., Ma, Y., & Zhou, Q. (2014). Effect of GO nanosheets on shapes of cement hydration crystals and their formation process. *Construction and Building Materials*, 64, 231-239.

- Lv, S., Ma, Y., Qiu, C., Sun, T., Liu, J., & Zhou, Q. (2013). Effect of graphene oxide nanosheets of microstructure and mechanical properties of cement composites. *Construction and building materials*, *49*, 121-127.
- Meng, W., & Khayat, K. H. (2016). Mechanical properties of ultra-high-performance concrete enhanced with graphite nanoplatelets and carbon nanofibers. *Composites Part B: Engineering*, *107*, 113-122.
- Meng, W., & Khayat, K. H. (2018). Effect of graphite nanoplatelets and carbon nanofibers on rheology, hydration, shrinkage, mechanical properties, and microstructure of UHPC. *Cement and Concrete Research*, *105*, 64-71.
- Mokhtar, M. M., Abo-El-Enein, S. A., Hassaan, M. Y., Morsy, M. S., & Khalil, M. H. (2017). Mechanical performance, pore structure and micro-structural characteristics of graphene oxide nano platelets reinforced cement. *Construction and Building Materials*, *138*, 333-339.
- Montes-Navajas, P., Asenjo, N. G., Santamaría, R., Menendez, R., Corma, A., & García, H. (2013). Surface area measurement of graphene oxide in aqueous solutions. *Langmuir*, *29*(44), 13443-13448.
- Novoselov, K. S., Fal, V. I., Colombo, L., Gellert, P. R., Schwab, M. G., & Kim, K. (2012). A roadmap for graphene. *nature*, *490*(7419), 192-200.
- Novoselov, K. S., Geim, A. K., Morozov, S. V., Jiang, D. E., Zhang, Y., Dubonos, S. V., ... & Firsov, A. A. (2004). Electric field effect in atomically thin carbon films. *science*, *306*(5696), 666-669.

- Pan, Z., He, L., Qiu, L., Korayem, A. H., Li, G., Zhu, J. W., ... & Wang, M. C. (2015). Mechanical properties and microstructure of a graphene oxide–cement composite. *Cement and Concrete Composites*, 58, 140-147.
- Papanikolaou, I., de Souza, L. R., Litina, C., & Al-Tabbaa, A. (2021). Investigation of the dispersion of multi-layer graphene nanoplatelets in cement composites using different superplasticiser treatments. *Construction and Building Materials*, 293, 123543.
- Peigney, A., Laurent, C., Flahaut, E., Bacsá, R. R., & Rousset, A. (2001). Specific surface area of carbon nanotubes and bundles of carbon nanotubes. *Carbon*, 39(4), 507-514.
- Qureshi, T. S., & Panesar, D. K. (2020). Nano reinforced cement paste composite with functionalized graphene and pristine graphene nanoplatelets. *Composites Part B: Engineering*, 197, 108063.
- Rahal, K. N., & Rumaih, H. A. (2011). Tests on reinforced concrete beams strengthened in shear using near surface mounted CFRP and steel bars. *Engineering Structures*, 33(1), 53-62.
- Raki, L., Beaudoin, J., Alizadeh, R., Makar, J., & Sato, T. (2010). Cement and concrete nanoscience and nanotechnology. *Materials*, 3(2), 918-942.
- Senff, L., Hotza, D., Lucas, S., Ferreira, V. M., & Labrincha, J. A. (2012). Effect of nano-SiO₂ and nano-TiO₂ addition on the rheological behavior and the hardened properties of cement mortars. *Materials Science and Engineering: A*, 532, 354-361.

- Sharma, S., & Arora, S. (2018). Economical graphene reinforced fly ash cement composite made with recycled aggregates for improved sulphate resistance and mechanical performance. *Construction and Building Materials*, 162, 608-612.
- Sixuan, H. (2012). Multifunctional graphite nanoplatelets (GNP) reinforced cementitious composites. *Master's Theses, National University of Singapore, Singapore, Singapore*.
- Stankovich, S., Dikin, D. A., Dommett, G. H., Kohlhaas, K. M., Zimney, E. J., Stach, E. A., ... & Ruoff, R. S. (2006). Graphene-based composite materials. *nature*, 442(7100), 282-286.
- Stynoski, P., Mondal, P., & Marsh, C. (2015). Effects of silica additives on fracture properties of carbon nanotube and carbon fiber reinforced Portland cement mortar. *Cement and Concrete Composites*, 55, 232-240.
- Tong, T., Fan, Z., Liu, Q., Wang, S., Tan, S., & Yu, Q. (2016). Investigation of the effects of graphene and graphene oxide nanoplatelets on the micro-and macro-properties of cementitious materials. *Construction and Building Materials*, 106, 102-114.
- Tragazikis, I. K., Dassios, K. G., Dalla, P. T., Exarchos, D. A., & Matikas, T. E. (2019). Acoustic emission investigation of the effect of graphene on the fracture behavior of cement mortars. *Engineering Fracture Mechanics*, 210, 444-451.
- Wang, B., & Zhao, R. (2018). Effect of graphene nano-sheets on the chloride penetration and microstructure of the cement based composite. *Construction and Building Materials*, 161, 715-722.

- Wang, B., & Zhao, R. (2018). Effect of graphene nano-sheets on the chloride penetration and microstructure of the cement based composite. *Construction and Building Materials*, 161, 715-722.
- Watanabe, K., Kimura, T., & Niwa, J. (2010). Synergetic effect of steel fibers and shear-reinforcing bars on the shear-resistance mechanisms of RC linear members. *Construction and Building Materials*, 24(12), 2369-2375.
- Yu, M. F., Lourie, O., Dyer, M. J., Moloni, K., Kelly, T. F., & Ruoff, R. S. (2000). Strength and breaking mechanism of multiwalled carbon nanotubes under tensile load. *Science*, 287(5453), 637-640.
- Zheng, Q., Han, B., Cui, X., Yu, X., & Ou, J. (2017). Graphene-engineered cementitious composites: small makes a big impact. *Nanomaterials and Nanotechnology*, 7, 1847980417742304.
- Zhu, Y., Murali, S., Cai, W., Li, X., Suk, J. W., Potts, J. R., & Ruoff, R. S. (2010). Graphene and graphene oxide: synthesis, properties, and applications. *Advanced materials*, 22(35), 3906-3924.
- Zohhadi, N. (2014). Functionalized graphitic nanoreinforcement for cement composites.

APPENDIX A

SUPPORTING MATERIAL FOR CHAPTER 4

Table A.1 Compression test results for all specimens of different batches

Specimen	G dosage (% BWOC)	Compressive Strength (MPa)
CS1	0	29.8
CS2	0	31.8
CS3	0	30.5
CS4	0	32.2
CS5	0	34
SG1 1	0.01	37.3
SG1 2	0.01	36.2
SG1 3	0.01	37.7
SG1 4	0.01	38.4
SG1 5	0.01	38.0
SG1 6	0.01	34.7
SG2 1	0.02	42.1
SG2 2	0.02	39.1
SG2 3	0.02	42.5
SG2 4	0.02	45.8
SG2 5	0.02	42.7
SG2 6	0.02	39.2
SG3 1	0.03	42.9
SG3 2	0.03	44.8
SG3 3	0.03	43.9
SG3 4	0.03	41.4
SG3 5	0.03	46.8
SG3 6	0.03	42.3
SG4 1	0.04	38.0
SG4 2	0.04	39.0
SG4 3	0.04	38.5
SG4 4	0.04	36.3
SG4 5	0.04	38.0
SG4 6	0.04	43.0

BG1 1	0.01	36.6
BG1 2	0.01	37.7
BG1 3	0.01	38.5
BG1 4	0.01	37.9
BG1 5	0.01	36.6
BG1 6	0.01	33.7
BG2 1	0.02	41.1
BG2 2	0.02	41.9
BG2 3	0.02	39.3
BG2 4	0.02	39.8
BG2 5	0.02	38.9
BG2 6	0.02	42.0
BG3 1	0.03	42.1
BG3 2	0.03	39.8
BG3 3	0.03	43.3
BG3 4	0.03	43.0
BG3 5	0.03	39.7
BG3 6	0.03	46.0
BG4 1	0.04	41.6
BG4 2	0.04	41.1
BG4 3	0.04	37.2
BG4 4	0.04	40.3
BG4 5	0.04	39.4
BG4 6	0.04	38.7

*CS is the control batch (reference) with no addition of graphene

*(S or B) refer to the method used for graphene dispersion, (S) for the ultrasonication, and (B) for the mechanical blending.

*G refers to the addition of graphene.

Table A.2 Cost of the materials

Material	Cement	Sand	Graphene(G)	PC	Ultrasonication
Cost	0.55 \$/kg	0.29 \$/kg	5000 \$/kg	10 \$/kg	5 \$/hour